





High-resolution dielectric anisotropy investigation of carbon nanotube–smectic-*A* liquid crystal dispersions: An upper limit of the latent heat and the pretransitional anomaly at the nematic–smectic-*A* transition

Funda Guven , Ozgun Girgin , Mehmet Can Cetinkaya, Haluk Ozbek , and Sevtap Yildiz ^{*}
Department of Physics, Istanbul Technical University 34469 Maslak, Istanbul, Turkey



(Received 12 October 2022; accepted 1 February 2023; published 14 February 2023)

Within the entire mesomorphic range, high-precision dielectric anisotropy data with the high-temperature resolution is presented for a highly polar smectic-*A* liquid crystal 8CB (octylcyanobiphenyl) as well as 8CB nanocomposites doped with both pristine multi-walled carbon nanotubes (p-MWCNTs) and carboxyl group (-COOH) functionalized MWCNTs (f-MWCNTs). The temperature variation of the nematic order parameter across both the nematic-isotropic (N-I) and the nematic–smectic-*A* (N-Sm-*A*) phase transitions of the neat 8CB and 8CB+MWCNT nanocomposites has then been derived from the dielectric anisotropy data within the framework of the Maier-Meier theory. With the inclusion of MWCNTs, both the N-I and the N-Sm-*A* transition temperatures have been noted to shift to lower temperatures as compared to the 8CB host. Also, for all 8CB+MWCNT nanocomposites, regardless of the surface functionalization, it has been well documented that the N-I transition is weakly first order, whereas the N-Sm-*A* transition remains continuous within the experimental resolution. For all investigated samples, the temperature dependence of the nematic order parameter has been shown to be quasitricritical, within the experimental resolution. From the attentive inspection of the dielectric anisotropy data in the vicinity of the N-Sm-*A* transition, the upper limits for a possible latent heat ΔH_{NA} for the 8CB host and all 8CB+MWCNT composites, for the first time, have been derived. The so-derived ΔH_{NA} values for all investigated samples have also been compared with those extracted from the optical birefringence data, and an excellent consistency has then been noted. The N-Sm-*A* pretransitional anomaly has been investigated and the effective specific heat capacity exponent α values have been yielded from the power-law analysis of our high-resolution $\Delta\varepsilon(T)$ data across the N-Sm-*A* transition for all investigated samples. It has been well documented that the incorporation of MWCNTs to the 8CB host leaves the N-Sm-*A* transition essentially bulklike. We discussed that, to some extent, the compliance of MWCNTs does not drive the N-Sm-*A* transition to 3D-XY-like behavior, that is the strength of de Gennes coupling will remain the same for all nanocomposites. This issue can be ascribed to the weaker nature of MWCNT disorder. In this work, for the first time, high-resolution $\Delta\varepsilon(T)$ data has been shown to be very adequate and offer an easy way to investigate the N-Sm-*A* transition as compared to calorimetric methods.

DOI: [10.1103/PhysRevE.107.024702](https://doi.org/10.1103/PhysRevE.107.024702)

I. INTRODUCTION

Liquid crystalline phases, i.e., mesophases, are known to be characterized by orientational order while the positional order has disappeared or is reduced to some extent. Those mesophases exhibit intermediate physical properties in between the isotropic liquid (I) and the three-dimensionally ordered solid. Two of the most extensively studied phases, both experimentally and theoretically, are the nematic (N) and the smectic-*A* (Sm-*A*) phases for thermotropic liquid crystals (LCs). In the orientationally ordered nematic phase, with the absence of positional order, the molecules tend to point in the same direction, the so-called director. Besides the orientational order, the smectic-*A* exhibits partial positional order with that the molecules are arranged in layers [1,2]. Moreover, in recent years, a substantial interest has been drawn to the inclusion of various types of nanomaterials, such as

nanoparticles (NPs), carbon nanotubes (CNTs), quantum dots (QDs), and also nanowires, to LCs for various electro-optical applications especially due to their gray-scale capabilities as well as due to elastic-mediated interactions between the LC host and aforesaid nanomaterials. Up to date, the dispersion of those nanomaterials in LCs has been shown to influence and improve their structural, mechanical, viscoelastic, electro-optical, and dielectric properties ([3–9] and references cited therein). Also, large mechanical stiffness, large electrical conductivity anisotropy, and huge aspect ratio together with the shape compatibility to LCs raise CNTs as promising materials from both technological and scientific aspects among the abovementioned nanomaterials. Hence, more recently, many studies have been devoted to this issue ([10–16] and references cited therein).

Additionally, regarding the scientific standpoint, LCs have been well documented as appealing model systems for testing the general concepts of phase transitions, particularly the first- or second-order (continuous) character of the transition as well as the universality of the associated critical

^{*}sevtap@itu.edu.tr

phenomena [2,17–19]. To date, the N-Sm-A transition has probably been one of the most exhaustively studied but at the same time is the most controversial transition since there exists no consensus between theory and experiments and between one experimental method and the other as well [2,17,19–21]. Various experimental studies have revealed nonuniversal critical behavior ([2,21] and references cited therein). Within the mean-field approximation, theories to date advocated that the N-Sm-A transition exhibits a crossover behavior from the 3D-XY-like second order to the first order via a Gaussian tricritical point (TCP) by assuming the coupling between the N and the Sm-A order parameters, the so-called de Gennes coupling [1,2,17]. As also demonstrated experimentally ([2,21] and references cited therein), the strong coupling, which corresponds to a narrow N range, gives rise to a first-order N-Sm-A transition, while the weak coupling, claiming a wide N range, yields a second-order (continuous) transition. However, it was subsequently claimed by Halperin, Lubensky, and Ma (HLM) [22,23] that if a finite coupling between the nematic director fluctuations and the Sm-A order parameter is taken into account, in analogy with type-I superconductors, then the transition is always weakly first order.

During the past four decades, the aforementioned theoretical predictions have been experimentally tested via various high-resolution methods, especially for alkylcyanobiphenyl (nCB) and alkyloxycyanobiphenyl (nOCB) homologs as well as their binary mixtures [21,24–26], because those are known to be photochemically stable and also to combine low melting points with reasonably high nematic-LC transition points [27]. In this regard, as a well-characterized LC, exhibiting I-N-Sm-A polymorphism, the 8CB (octylcyanobiphenyl) compound is the most representative one, from both fundamental and applicational perspectives. To date, any evidence for a first-order character of the N-Sm-A transition for 8CB has been revealed neither calorimetrically [28] nor optically [29]. Moreover, in literature, one can find out high-resolution calorimetric studies concerning the influence of different type nanomaterials such as BaTiO₃ [30], CdS [31], CdSe NPs [32] as well as magnetic NPs with different surface coatings [33] on the phase transition characteristics of the 8CB LC host. Additionally, Mertelj *et al.* reported optical birefringence data of 8CB+BaTiO₃ nanocomposites to understand the impact of those NPs on the N-Sm-A transition [34] and recently, a correlation between dielectric properties and phase transitions of 8CB+Sn₂P₂S₆ nanocomposites has been presented as well [35]. However, in the past, a calorimetric study on the phase transitions of 8CB+MWCNT nanocomposites (MWCNT refers here to multi-walled carbon nanotube) was presented by Sigdel and Iannacchione [36]. Very recently, high-resolution optical birefringence measurements of 8CB+MWCNT nanocomposites were presented by our group [37].

Nonetheless, regarding experimental techniques, particularly interesting are static dielectric permittivity studies since they are known to be not only a crucial parameter characterizing the response of the LC medium to the external electric field but also directly proportional, via dielectric anisotropy, to the nematic (orientational) order parameter itself [38]. Also, it is of fundamental interest to know the temperature behavior of the nematic order parameter to test any model of liquid

crystalline behavior [39]. As far as the phase transitions of LC+nanomaterial composites are concerned, static dielectric permittivity and high-resolution dielectric anisotropy studies, which are utilized to probe the behavior of the nematic order parameter especially in the vicinity of the N-Sm-A transition, have still been quite surprisingly limited [40,41]. In the past, the pretransitional behavior only in the vicinity of the N-I transition of 5OCB+BaTiO₃ [40] and the I-Sm-A transition of 12CB+BaTiO₃ [41] nanocomposites were studied via static dielectric permittivity measurements. The evidence for the pretransitional behavior seen in dielectric properties for different liquid crystalline systems, especially across the N-Sm-A transition, still seems quite limited. Thus, due to the lack of those kind studies, we report, in this work, high-resolution dielectric anisotropy measurements covering the N and the Sm-A phases of both 8CB and 8CB+MWCNT nanocomposites. We have derived the upper limit of the latent heat of the N-Sm-A transition by deducing the nematic order parameter from our dielectric anisotropy data, and finally, then, we have discussed the pretransitional anomaly related to this transition. Afterward, the comparison of the results with those by high-resolution optical birefringence data [37] is presented as well. To the best of our knowledge, apart from this work, there seems no systematic study documenting the upper limit of the latent heat of the continuous N-Sm-A transition deduced from high-resolution dielectric anisotropy data. It is noteworthy that, in the present paper, as dopants to the 8CB host, both pristine MWCNTs (p-MWCNT) and -COOH (carboxyl) group functionalized MWCNTs (f-MWCNT) have been utilized.

II. THEORETICAL BACKGROUND

A. Nematic order parameter and the nematic-isotropic transition

It is notable that the orientational order parameter, specifying the orientational distribution of the long molecular axis around the director, characterizes the long-range orientational order in LCs. Additionally, the uniaxial symmetry of both the N and Sm-A phases is known to result in anisotropic behavior for several physical quantities and hence, any anisotropic physical quantity can be a measure of orientational ordering in the N phase, as pointed out first by de Gennes [1]. As far as dielectric anisotropy $\Delta\epsilon$ ($\Delta\epsilon = \epsilon_{\parallel} - \epsilon_{\perp}$, with ϵ_{\parallel} and ϵ_{\perp} static dielectric permittivities along and perpendicular to the nematic director, respectively) measurements are concerned, one can pursue these high-resolution $\Delta\epsilon$ data to get an insight information on the degree of orientational order in the liquid crystalline phases. Particularly, the $\Delta\epsilon$ data can be used to investigate the temperature dependence of the N (orientational) order parameter $S(T)$. Recall that in the past, high-resolution optical birefringence data have successfully been used by our group to probe both the temperature behavior of the N order parameter and the pretransitional effects in the vicinity of both the N-I and the N-Sm-A transitions in several liquid crystalline systems, such as in pure LCs [29,42] and their binary mixtures [25,26] as well as some LC+nanomaterial composites [37,43]. In the present case, high-resolution $\Delta\epsilon$ data has been exploited to probe those pretransitional effects. Furthermore,

static dielectric permittivity, as well as dielectric anisotropy has been well documented by using the Maier-Meier theory [44], which is itself the extension of the Onsager theory to LCs. As per this theory, dielectric anisotropy $\Delta\varepsilon$ is given by

$$\Delta\varepsilon = \frac{NhF}{\varepsilon_0} \left[\Delta\gamma - \frac{F\mu^2}{2k_B T} (1 - 3\cos^2\varphi) \right] S, \quad (1)$$

where ε_0 is the permittivity of free space, k_B is the Boltzmann constant, T is the absolute temperature, $\Delta\gamma$ is the polarizability anisotropy, μ is the resultant dipole moment of the molecule, φ is the angle between the dipole and the long molecular axis, and N is the number density of molecules. Here F is the feedback factor and $h = 3\bar{\varepsilon}/(2\bar{\varepsilon} + 1)$ with $\bar{\varepsilon} = (\varepsilon_{\parallel} + 2\varepsilon_{\perp})/3$. Additionally, the polarizability anisotropy $\Delta\gamma$ is given as $\Delta\gamma = \gamma_{\parallel} - \gamma_{\perp}$, with γ_{\parallel} and γ_{\perp} longitudinal (parallel) and transverse (perpendicular) polarizabilities relative to the long molecular axis, respectively.

Besides, regarding the weakly first-order character of the N-I transition [45,46], through high-resolution data, a four-parameter generic power-law expression has recently been shown to well portray the temperature variation of $S(T)$. Also, by taking into account the scaling condition that the nematic order would be perfect at $T = 0$ K, as elsewhere [25,26,37,47,48], one can write down the $S(T)$ as follows:

$$S(T) = S^{**} + (1 - S^{**})|\tau|^{\beta}, \quad (2)$$

with $\tau = 1 - T/T^{**}$, here T^{**} refers to the effective second-order transition temperature, i.e., the spinodal temperature of the N phase, β is the critical exponent related to the fluctuations at the N-I transition T_{IN} . Thus, $\Delta T^{**} = T^{**} - T_{IN}$ is the temperature metric of the discontinuity of the N-I transition, which is still one issue for debate. Then, combining Eqs. (1) and (2) and also considering only the explicit temperature dependence seen in those equations allows one to describe the temperature variation of $\Delta\varepsilon(T)$ as

$$\Delta\varepsilon = \left(C_1 + \frac{C_2}{T} \right) [S^{**} + (1 - S^{**})|\tau|^{\beta}], \quad (3)$$

where the constants C_1 and C_2 are given by

$$C_1 = \frac{NhF}{\varepsilon_0} \Delta\gamma, \quad (4a)$$

$$C_2 = -\frac{NhF^2\mu^2}{2\varepsilon_0 k_B} (1 - 3\cos^2\varphi). \quad (4b)$$

Thereby, the N order parameter $S(T)$ can be deduced directly from the $\Delta\varepsilon(T)$ data, by utilizing the following relation:

$$S(T) = \frac{\Delta\varepsilon(T)}{\left(C_1 + \frac{C_2}{T} \right)}. \quad (5)$$

To further check the validity of Eq. (5), we have then used the $S(T)$ data extracted from the optical birefringence Δn data given in Refs. [49] and then compared it with the one deduced via Eq. (5) for pure pentylcyanobiphenyl (5CB) LC. We have then observed a good agreement between those $S(T)$ values with that typical error is 1.5% over the entire temperature range investigated. As will be discussed herein below, Eqs. (3) and (5) will be used in deriving the N order parameter and

also upper limit of the latent heat ΔH_{NA} for the continuous N-Sm-A transition of the 8CB host and 8CB+MWCNT composites and then also used for the comparison with the previously published results, obtained from optical measurements [29,37]. We must remark here that during the past few decades, in literature, the so-called fluidlike model has thoroughly been exploited to quantify the temperature dependence of the static dielectric permittivity in the vicinity of the N-I transition of rodlike LC molecules, whose permanent dipole moments are approximately parallel to their long axes, as in the case of 8CB [40,41,50–55]. We must notice here that, in the abovementioned studies, the nematic order parameter $S(T)$ was not derived from the $\Delta\varepsilon$ data presented and neither any latent heat values ΔH_{NA} nor the pretransitional effects were also addressed for the samples exhibiting the N-Sm-A transition. However, unlike the “fluidlike” model presented in Refs. [40,41,50–55], in this work for the first time, we have deduced the order parameter $S(T)$ via Eq. (5) based on the Maier-Meier theory and then we have used it to produce the latent heat values of the samples under investigation. Besides, in the past, although Thoen and Menu presented an expression very similar to Eq. (3) to quantify their $\Delta\varepsilon$ data for the 8CB host [56], no value for the latent heat in the vicinity of the N-Sm-A transition was addressed by the authors of Ref. [56].

Apart from the N-Sm-A transition, the N-I transition seems to be a subject of various studies both experimentally and theoretically [2,18,21,38]. The nature of the N-I transition is shown to be weakly first order with a small latent heat and substantial pretransitional fluctuation effects have also been well documented [2,18,21]. Additionally, the critical exponent values obtained from various physical quantities near the transition are shown to be in line with the tricritical hypothesis (TCH) [45,57]. Moreover, the simplest description of the thermodynamic behavior of the N-I transition is given by phenomenological Landau–de Gennes mean-field theory [17,18]. It is worth noting that the tricritical hypothesis with this transition was first conjectured by Keyes [57] and it was shown within the mean-field approach by assuming a sixth-order term in the Landau–de Gennes free-energy expansion [45,58]. Hence, for a uniaxial nematic LC, as in the case of 8CB, the nematic free-energy density F_N can be written as an expansion of the powers of the nematic order parameter S as follows:

$$F_N = F_I + \frac{1}{2}A_N S^2 - \frac{1}{3}B_N S^3 + \frac{1}{4}C_N S^4 + \frac{1}{6}E_N S^6, \quad (6)$$

where F_I is the free-energy density in the isotropic phase. The temperature-dependent coefficient A_N is assumed to be $A_N = \left(\frac{a_0}{T_{IN}}\right)(T - T^*)$ with $a_0 > 0$ and T^* the lower stability limit of the isotropic phase. The constant $B_N > 0$ makes the N-I transition first order and its value can be reduced by molecular biaxiality [58,59]. However, by focusing on the N-I transition near the tricritical point, one can proceed as follows. As the tricritical phase transition is approached, the coefficient B_N is getting smaller, so it can be neglected and the coefficient C_N is taken to be small and negative as discussed elsewhere [58]. Thus, by following up the strategy given by Salud *et al.* [58] and taking $B_N = 0$ and $C_N = -C_0$ with $C_0 > 0$, the finite discontinuity in the nematic order parameter at T_{IN} , viz.

S_{IN} , and also the entropy discontinuity $\Delta\bar{S}_{IN}$ at T_{IN} can be obtained as

$$S_{IN} = \sqrt{\frac{3C_0}{4E_N}}, \quad (7a)$$

$$\Delta\bar{S}_{IN} = \frac{3a_0C_0}{8T_{IN}E_N} = \frac{a_0S_{IN}^2}{2T_{IN}} = \frac{\Delta H_{IN}}{T_{IN}}, \quad (7b)$$

with ΔH_{IN} the latent heat at the N-I transition.

B. The Nematic–Smectic-A Transition

Since the Sm-A phase is characterized by a two-component, a magnitude Ψ , and a phase ϕ order parameter, the isotropic 3D-XY model would be expected to be the simplest model for the N-Sm-A transition. But, as briefly discussed in Sec. I, the nature of this transition is rather complicated due to the presence of some deviations from the isotropic 3D-XY behavior. The first type of deviation is due to the coupling, namely the de Gennes coupling, between the N and the Sm-A order parameters and it results in the crossover from second-order in nature to first order via a TCP. The second type of deviation is due to the coupling between the nematic director fluctuations and the Sm-A order parameter (*viz.* $\delta\hat{n} - \Psi^2$ coupling) and gives rise to very weakly first-order N-Sm-A transition. However, regarding the 8CB LC, high-resolution calorimetric [28] and optical [29] methods have well documented a continuous N-Sm-A transition. Thus, for discussing the pertinent thermodynamic description of this transition, only the de Gennes coupling term seems enough to include in the free-energy density of the Sm-A phase, yielding in the following form:

$$F = F_N + \frac{1}{2}a_A(T - T_{NA})\Psi^2 + \frac{1}{4}b_A\Psi^4 + \frac{1}{6}d_A\Psi^6 - c_A\Psi^2\delta S + \frac{1}{2\chi_N}(\delta S)^2, \quad (8)$$

with the expansion coefficients (a_A, b_A, d_A, c_A) > 0 and here T_{NA} refers to the N-Sm-A transition temperature. Also, δS represents here the extra nematic order due to the presence of the smectic layering, while χ_N is the nematic susceptibility, whose value depends on the nematic temperature range NR (NR = $T_{IN} - T_{NA}$) and is larger in the vicinity of T_{IN} as well. From the minimization with respect to δS one can get $\delta S = c_A\chi_N\Psi^2$, then upon elimination of δS from F reads

$$F = F_N + \frac{1}{2}a_A(T - T_{NA})\Psi^2 + \frac{1}{4}b'_A\Psi^4 + \frac{1}{6}d_A\Psi^6, \quad (9)$$

with $b'_A = b_A - 2c_A^2\chi_N$. Notice that if χ_N is small, which results in a wide N range, then $b'_A > 0$, and a continuous N-Sm-A transition occurs. As χ_N grows, the point $b'_A = 0$ is reached which corresponds to TCP. For larger χ_N where $b'_A < 0$, giving rise to a narrow N range, the N-Sm-A transition is of first order. Finally, by taking into account the free-energy densities given in Eqs. (6) and (9) and also by following the steps, whose details were published in our previous work [29], a relationship between the entropy change $\Delta\bar{S}$ and the nematic order parameter change ΔS_{NA} in the immediate vicinity of the

N-Sm-A transition T_{NA} will be given as

$$\Delta\bar{S} = \frac{a_0}{T_{IN}}S_{NA}\Delta S_{NA}, \quad (10)$$

where $S_{NA} = [S_A(T_{NA}) + S_N(T_{NA})]/2$ and $\Delta S_{NA}(T_{NA}) = S_A - S_N$. In this way, one can obtain the latent heat for the first-order (discontinuous) N-Sm-A transitions as well as the upper limit of the latent heat for the second-order (continuous) N-Sm-A transitions via the following expression:

$$\Delta H_{NA} = T_{NA}\Delta\bar{S} = a_0R_M S_{NA}\Delta S_{NA}, \quad (11)$$

with $R_M = T_{NA}/T_{IN}$, the so-called McMillan ratio. Notice that as discussed elsewhere [29], the forms of Eqs. (10) and (11) are valid also within the framework of the HLM theory. To date, the usage of Eq. (11) has successfully been tested solely via high-resolution optical birefringence measurements for several liquid crystalline systems [25,26,29,37,43]. Hence, in this work for the first time, as far as we know, we have discussed its validity via high-resolution dielectric anisotropy $\Delta\epsilon$ measurements for both 8CB host and 8CB+MWCNT composites.

III. METHODOLOGY

A. Samples

The smectic-A LC host 8CB, with a molecular mass of 291.44 g/mol, (assay 99.8%) was procured from AWAT Co. Ltd., Warsaw, Poland, and no further purification was performed. Both unfunctionalized, namely pristine, and -COOH group surface functionalized MWCNTs (with a nominal purity of 98%) have 5-8 nm in diameter and 1–5 μm in length and they were kindly donated by BAYER, Germany. We have prepared both 8CB-f-MWCNT and 8CB-p-MWCNT composites by solvent dispersion method, details of which can be found elsewhere [37,60–63]. We have prepared two different types of 8CB+MWCNT dispersions with MWCNT mass fractions χ of 0.007 and 0.07. We must note here that, for comparison purposes, both p-MWCNT and f-MWCNT contents in this work were chosen to be the same as those of MWCNTs given in our previous studies [37,62,63]. Also, for the ease of presentation, gathered in Table I are the sample codes used throughout this work and the properties of the samples used in the experiments.

B. Experimental methods

The temperature-dependent static dielectric permittivity ϵ measurements were conducted at a frequency of 10 kHz and at a probing voltage of 0.3 V_{rms} via a GW-Instek Model 8110-G precision LCR meter with a relative accuracy of 0.1%. It is imperative to note that this frequency is out of the region of the dielectric relaxation of the LC and no dispersion was reported up to 100 kHz as well [56,60,64]. Additionally, at this frequency, MWCNTs have been reported not to exhibit space charge or dipole orientation dynamics [60,61]. During the static dielectric permittivity measurements, the temperature was measured and controlled by means of an RTD sensor (Omega Eng. Corp.) and a Lake Shore Model 335 temperature controller with a resolution and measured stability of 0.001 K. Of note, during data acquisition, the temperature

TABLE I. Codes and properties of the samples under investigation in this work.

Sample	Mass fraction of MWCNT χ	Surface functionalization of MWCNT
8CB host	0	—
p-0.007	0.007	None (pristine)
p-0.07	0.07	None (pristine)
f-0.007	0.007	carboxyl group (-COOH)
f-0.07	0.07	carboxyl group (-COOH)

step was 4 mK, and also the waiting times were always larger than 60 s until the temperature stability (within 0.001 K) was achieved. We stress here that all ε measurements were carried out upon cooling since the better alignment of LCs is expected to be better than that in heating cycles. Furthermore, that the whole setup is fully computerized and runs under a LabVIEW (National Instruments) must be noted. It must be stressed that to check the accuracy of our ε measurements, the dielectric constants of 5CB LC compound have also been measured via our set-up and the close agreement with the reported values [65,66] in literature was achieved. The high-resolution permittivities ε_{\parallel} and ε_{\perp} along and perpendicular to the director, respectively, were obtained by measuring the capacitance of appropriately aligned sample cells, details of which can be found elsewhere [62,63]. Further details on the preparation of appropriately aligned sample cells were also described in Refs. [62,63], while the alignment check procedure and the cell thickness test were discussed elsewhere [42]. Henceforth, no more detailed explanation of those issues will be given. Prior to measurements, the structure of all MWCNT-doped samples was observed under polarizing microscope (POM). Textures of the samples were homogeneous and similar to that of the 8CB host, indicating a uniform nematic director field, as presented previously [62]. Thus, concluding is that both p-MWCNT and f-MWCNTs are uniformly dispersed and the inclusion of them does not exhibit any visible aggregation in the doped system [60–63,67].

IV. RESULTS AND DISCUSSIONS

A. Overview and the phase transition temperatures

The high-resolution dielectric anisotropy $\Delta\varepsilon$ measurements of both neat 8CB and 8CB+MWCNT blends have been performed over the temperature interval of $297\text{K} \leq T \leq 318\text{K}$. Our $\Delta\varepsilon(T)$ data were collected upon cooling from the isotropic liquid phase down to the Sm-A phase. Notice that, in literature, there exist several reports on dielectric measurements of the neat 8CB over the interval $295\text{K} \leq T \leq 333\text{K}$ ([56] and references cited therein). But, quite interestingly, none of those studies have yet reported on the upper limit of the latent heat of 8CB near the N-Sm-A transition based on their dielectric data, contrary to the present work. Illustrated in Fig. 1 is the overview of the thermal variation of our high-resolution $\Delta\varepsilon$ data as a function of the shifted temperature $T - T_{IN}$ for all investigated samples. One can notice that in the isotropic liquid phase of all investigated samples $\Delta\varepsilon$ is zero, confirming no long-range orientational order due to the absence of elastic interactions in the isotropic phase. Thus, one can consider the T_{IN} transition

temperatures to be the lowest temperature value corresponding to the zero dielectric anisotropy in the isotropic phase, as in the case of the optical birefringence measurements [25,26,43]. As seen in Fig. 1, all samples including the neat 8CB exhibit a large positive dielectric anisotropy, as expected, due to the presence of a strong dipole moment of the terminal

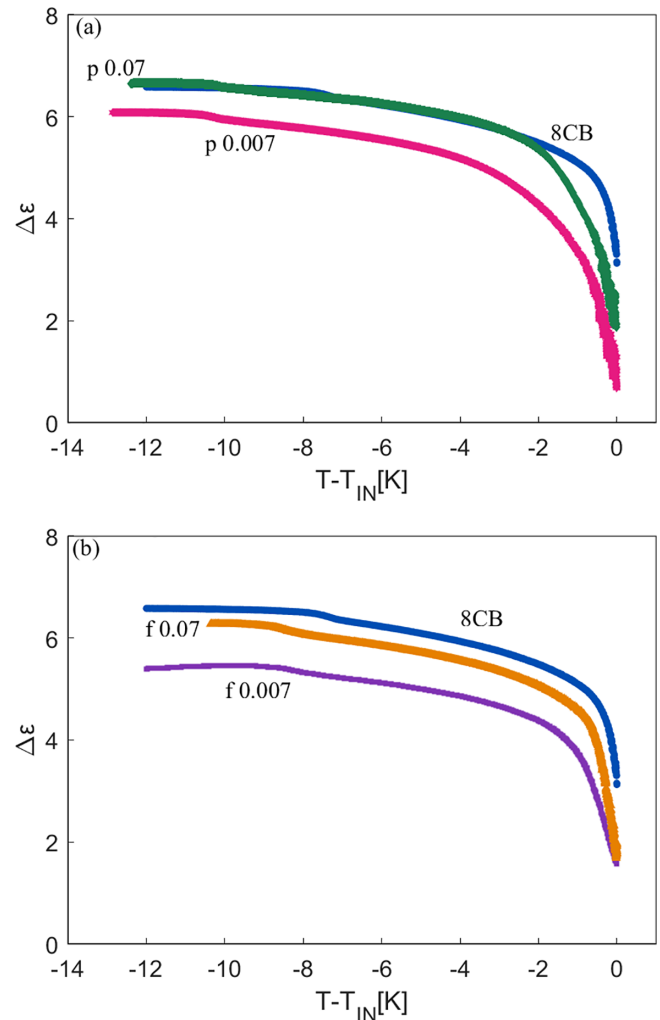


FIG. 1. Dielectric anisotropy $\Delta\varepsilon$ versus shifted temperature $T - T_{IN}$ (here, T_{IN} is the N-I transition temperature of the related sample) for (a) the 8CB host and 8CB+pMWCNT nano composites and (b) the 8CB host and 8CB+f-MWCNT nano composites. Note that in the figures, p refers to pristine-unfunctionalized-MWCNTs, while f refers to -COOH functionalized MWCNTs. Different MWCNT contents χ for both p-MWCNT and f-MWCNT dopants are disclosed in the figures.

TABLE II. Overview of the thermal behavior of the neat 8CB and 8CB+MWCNT blends produced from the high-resolution $\Delta\varepsilon$ data. Presented are the change in the phase transition temperature ΔT_{IN} , T_{NA} of the 8CB+MWCNT system with respect to those of the 8CB host. Here, $\Delta T_{IN} = T_{IN} - T_{IN}^0$ and $\Delta T_{NA} = T_{NA} - T_{NA}^0$ represent the shifts of the N-I and the N-Sm-A transition temperatures, respectively. T_{IN}^0 and T_{NA}^0 refer to the N-I and the N-Sm-A transition temperatures of the neat 8CB. Also shown are the nematic phase temperature range NR ($NR = T_{IN} - T_{NA}$), the upper limit of the latent heat ΔH_{NA} across T_{NA} , so obtained under atmospheric pressure, and the extracted effective critical exponent α via Eq. (19) for 8CB+MWCNT blends as well as the 8CB host. For the meaning of the abbreviations appearing in the first column, please refer to Table I. The N-I and N-Sm-A phase transition temperatures of the neat 8CB are $T_{IN}^0 = 313.37\text{K}$ and $T_{NA}^0 = 306.11\text{K}$.

Sample	ΔT_{IN} [K]	ΔT_{NA} [K]	NR [K]	ΔH_{NA} [J/kg]	α
8CB host	0	0	7.26	3.03 ± 0.30	0.3214 ± 0.0003
p-0.007	-3.05	-5.93	10.14	8.97 ± 0.85	0.3217 ± 0.0001
p-0.07	-3.82	-6.74	10.18	8.85 ± 0.60	0.3220 ± 0.0008
f-0.007	-1.88	-2.83	8.21	7.75 ± 0.60	0.3220 ± 0.0002
f-0.07	-1.34	-2.49	8.41	9.70 ± 0.80	0.3218 ± 0.0012

-CN group ($\approx 5D$), oriented along the long molecular axis in nCB homologs [1,38,52]. After a discernible change at T_{IN} , for the neat and all MWCNT-doped 8CB samples, $\Delta\varepsilon(T)$ grows up with decreasing temperature due to the increase in the orientational order over the entire nematic phase. For all samples, with further decreasing temperature toward the Sm-A phase, a substantial increment in $\Delta\varepsilon(T)$ takes place, since the quasi-long-range order (the phrase ‘‘quasi’’ is because of the Landau-Peierls instability [1]) in the Sm-A mesophase builds up, signaling the growth of one-dimensional positional order together with the orientational order [1,7,20]. But it is notable that the temperature variation of $\Delta\varepsilon(T)$ in the Sm-A phase seems more sluggish as compared to the N phase. Recalling that one can attribute this increment in $\Delta\varepsilon(T)$, accordingly in $S(T)$, to the better packing of the molecules in the smectic-A phase and an associated density effect as well [20]. Thus, we have precisely located the N-Sm-A transition temperatures T_{NA} , for all samples, as the peak temperature of the local slope $D_\varepsilon(T)$ [$D_\varepsilon = -d(\Delta\varepsilon)/dT$], by following up on the literature [53,54,68–71]. In Table II, we have summarized our experimental findings concerning the thermal behavior of both 8CB+p-MWCNT and 8CB+f-MWCNT composites together with the neat 8CB, extracted from our high-resolution $\Delta\varepsilon(T)$ data. We emphasize here that the T_{IN} and T_{NA} phase transition temperatures of all MWCNT-doped 8CB samples were also determined from different techniques and previously presented elsewhere [37,62,63]. The changes in the transition temperatures extracted from our $\Delta\varepsilon(T)$ data relative to those produced from the other methods were 2% and 4% on average for the T_{IN} and T_{NA} temperatures, respectively. Also, for the neat 8CB, the T_{IN} and T_{NA} temperatures are in good agreement with the reported values via high-resolution a.c. calorimetry [30]. It is apparent from Table II that the inclusion of both types of MWCNTs, namely p-MWCNTs and f-MWCNTs to 8CB induces downward shifts in the T_{IN} and T_{NA} phase transition temperatures by demonstrating a nonlinear χ dependence. Also notice that a nearly 20% change, on average, in the nematic temperature range NR ($NR = T_{IN} - T_{NA}$) for the 8CB+MWCNT composites, is indicative of no substantial suppression of the orientational ordering relative to the smectic order due to the inclusion of MWCNTs [31]. The widths of the nematic temperature range for all samples including the 8CB host were found to be in good agreement with the those obtained via high-resolution optical birefringence data

within the experimental uncertainties [37]. Those downward shifts raise the fact that, in the composites, the surface distribution of p-MWCNT and f-MWCNTs for the 8CB host yields disordering and dilution effects from the elastic forces, which usually tends to decrease the transition temperatures. For the MWCNT-content regime studied here, presumably the floating of MWCNTs in the LC host medium rather produces disordering effects, resulting in a decrease in transition temperatures. We also emphasize that, as seen in Table II, the T_{NI} and T_{NA} temperatures of 8CB+p-MWCNT blends decrease at a higher rate relative to those of 8CB+f-MWCNT samples, which might be probably due to the effect of -COOH surface functionalization [62,63,72]. Furthermore, hydrogen bonding is also well known to be possible between the cyano group of 8CB LC and the -COOH functionalization group of MWCNT [62]. Hence, this interaction may lead to an increase in the ordering of 8CB+MWCNT composites as compared to the 8CB+p-MWCNT system. At this stage, to get more insight into the depression of the phase transition temperatures with the inclusion of MWCNT, it would be reasonable to focus on the changes in the transition temperatures with respect to those of the 8CB host, namely $\Delta T_{IN} = T_{IN} - T_{IN}^0$ and $\Delta T_{NA} = T_{NA} - T_{NA}^0$. Here, T_{IN}^0 and T_{NA}^0 refer to the N-I and the N-Sm-A transition temperatures of 8CB (cf. Table II). At first glance, one can see that both ΔT_{IN} and ΔT_{NA} decrease for the 8CB+p-MWCNT system with increasing the dopant content χ . However, for the 8CB+f-MWCNT system, while the quantities ΔT_{IN} and ΔT_{NA} decrease first, cf. for the f-0.007 sample, then they start slightly to rise with increasing χ , but while still keeping lower than zero. For the f-0.07 sample f-MWCNTs could interact with each other via the 8CB host molecules, producing somehow an ordering effect as compared to p-MWCNT dopants. Thus, one can assert that due to the presence of p-MWCNTs, the local arrangement of 8CB is distorted, while the arrangement of the 8CB host seems less distorted to some extent with the inclusion of f-MWCNTs because of the surface treatment. A quite similar ΔT_{IN} behavior was reported in the 5OCB+BaTiO₃ system based on static dielectric permittivity measurements by Starzonek *et al.* [40] as well. Apart from those, since our 8CB+MWCNT samples are reported as uniform, namely in a dilute MWCNT regime, based on POM observations [62], the suppression seen in the phase transition temperatures could not be due to elastic distortions. Thus, if a phenomenological

theory is wanted to construct, one should keep in view the MWCNT-LC host interface energy as well in a Landau-type free-energy expansion. To achieve this, some surface disordering terms, like $W_1 S^2$ and $W_2 \Psi^2$ with $W_1, W_2 > 0$, must be added up in the free energy, which could affect the T_{IN} and T_{NA} transition temperatures [73–75]. Here, W_1 and W_2 refer surface disordering potentials leading to the nonlinear shifts in the transition temperatures. We must emphasize here that when bearing in mind quite different behaviors of the quantities ΔT_{IN} and ΔT_{NA} for p-MWCNT and f-MWCNT dopants, the W_1 and W_2 surface disordering potentials could also be different for p-MWCNTs and f-MWCNTs. In the recent, quite similar phenomenological theories were discussed for some LC+NP systems, with a nematic LC host, as well [40,76,77]. However, we remark here that even if the abovementioned terms are included in the free-energy density, the form of Eq. (11) will remain the same. However, the disordering mechanism in the 8CB+MWCNT system studied here seems still predominant due to the long alkyl chain of 8CB, as compared to the shorter-chain-length homologs. In the literature, in some very recent studies, similar considerable decreases in the phase transition temperatures have been reported for some dispersions of LC+carbon-based nanostructures and also some NPs dispersed in the 8CB host. Herein, we refer to some experimental studies on this issue; 8CB+p-MWCNT [36], 5CB+p-SWCNT [78,79], 8CB+GO (graphene oxide) [80], E_{5CN7} +f-MWCNT [81], 6CHBT (4-(trans-4'-n-hexylcyclohexyl)-isothiocyanatobenzoate)+f-MWCNT [82], 7OBA (4-(heptyloxy) benzoic acid)+GO [83], gold NPs, silver NPs and $\text{Sn}_2\text{P}_2\text{S}_6$ NPs, all of which are dispersed in the 8CB host [72,84]. Of note here is that E_{5CN7} refers to the eutectic mixtures of 5CB and 7CB LCs [13]. In addition, despite those numerous experimental studies, theoretical aspects regarding how changing the generic dopant (CNTs, NPs) features affect the LC host properties are still scarce. Even recently, by Monte Carlo simulations, Orlandi and coworkers [85] investigated how the addition of rodlike NPs, like CNTs, affects the resulting liquid crystalline behavior. A general decrease in the transition temperatures and also a reduction in the temperature variation of the LC orientational order were concluded. Additionally, similar conclusions have also been drawn by others via a computational study [86].

Eventually, this nonlinear change of the phase transition temperatures with χ might be due to the interfacial properties of the MWCNT surface and 8CB LC molecules, giving rise to the changes in $\Delta\varepsilon$ as well as the optical birefringence Δn [36,37,62,63,81,87]. Except those, as was also reported by several studies [7,72,83,88,89], it is apparent from Fig. 1, the dielectric anisotropy $\Delta\varepsilon$ of 8CB+MWCNT blends decreases as compared to that of the 8CB host over the entire temperature interval spanning the N and Sm-A phases. But for only the p-0.07 sample, the dielectric anisotropy $\Delta\varepsilon$ nearly equals that of the host. Furthermore, we could stress here that the substantial reduction observed in $\Delta\varepsilon$ for MWCNT-doped samples is caused by the decrease in ε_{\parallel} , however, the ε_{\perp} values demonstrate nearly the same values as that of the 8CB host [62,63]. This observation was reported for several types of LC-based nanocomposites as well in literature [7,72,78,82,90,91]. Reasonably, one can infer that the inclusion of MWCNTs in the 8CB host could result in the emergence of chains, then

being able to produce an anti-parallel dipole moment to the longitudinal dipole moment of the 8CB host as well. Hence, the effective dipole moment of the composite system diminishes leading to decreasing in ε_{\parallel} and accordingly also $\Delta\varepsilon$ values [7,62,82,90]. Additionally, as compared to the lower MWCNT-content composites, the increase in $\Delta\varepsilon$ values of both p-0.07 and f-0.07 blends could be attributed to the formation of an increased number of MWCNT-8CB-MWCNT capacitors, as outlined elsewhere [62,92]. We will not give further details on the aforementioned issues, since our main goal in this work is to produce the latent heats ΔH_{NA} values and to investigate the pretransitional anomaly across T_{NA} from our $\Delta\varepsilon(T)$ data.

B. The nematic order parameter, the nematic-isotropic transition, and the spinodal temperature of the nematic phase

In this subsection, we present the thermal variation of the nematic order parameter $S(T)$ produced from our high-resolution $\Delta\varepsilon(T)$ data and its limiting behavior in the vicinity of the N-I transition for both the neat 8CB and 8CB+MWCNT composites. Also, we discuss the spinodal temperatures T^{**} and the so-called the temperature metric of the discontinuity of the N-I transition, viz. $\Delta T^{**} = T^{**} - T_{IN}$, being still a puzzling issue, and then compare our results with the reported values based on different measurements. Moreover, the T^{**} temperature is known to be effectively used in magnetic birefringence and light scattering studies [1]. As a first step, our experimental $\Delta\varepsilon(T)$ data have been fitted to Eq. (3) with the free parameters C_1 , C_2 , S^{**} , T^{**} , and β . To probe the nematic order parameter, the analysis of our $\Delta\varepsilon(T)$ data has proceeded through a nonlinear least-squares fitting procedure, a subroutine of MATLAB, which has been used successfully up to date [42,43,49,63]. This fitting procedure is based on the so-called conjugate gradient technique, a detailed and comprehensive description of which was reported elsewhere [47,93,94]. Collected in Table III are the most significant fitting parameters obtained via Eq. (3). Also, since all samples exhibit the N-Sm-A transition, we have further checked the influence of the pretransitional Sm-A behavior in the N phase. We have then documented a distinguishable pretransitional smectic behavior in a region up to 3.1 K on average for 8CB+MWCNT blends above T_{NA} , whereas for the neat 8CB, the observed is a 2-K-wide pretransitional range. We must discuss here that for all samples, the reported pretransitional smectic behavior temperature ranges in this work agree well with the ones obtained by high-resolution optical birefringence $\Delta n(T)$ data previously [37]. However, it is imperative to recall that in Ref. [56], for the 8CB host, quite surprisingly, Thoen and Menu did not divulge any pretransitional smectic behavior during the fitting of their $\Delta\varepsilon(T)$ data to an equation similar to Eq. (3) presented in this work.

For the neat 8CB, the temperature metric of the discontinuity ΔT^{**} has been found to be 0.06 ± 0.01 K. For the sake of comparison, in literature, one can find some reported values for this metric ΔT^{**} for the neat 8CB based on various high-resolution measurements. In Ref. [56], Thoen and Menu reported that $\Delta T^{**} = 0.1$ K via $\Delta\varepsilon$ measurements. Besides, Zywockinski found $\Delta T^{**} \approx 0.11$ K via molar

TABLE III. Fitting parameter values extracted from the fitting of $\Delta\varepsilon$ data with Eq. (3) within the N phase of 8CB+MWCNT blends as well as the 8CB host. Of note is that T^{**} refers to the effective second-order phase transition temperature seen from below T_{IN} , and S^{**} is the value of the N order parameter at $T = T^{**}$. For the meaning of the abbreviations appearing in the first column, please see Table I.

Sample	C_1	C_2	S^{**}	$T^{**} - T_{IN}$ [K]	β
8CB host	22.50 ± 2.07	-3261.61 ± 135.50	0.2352 ± 0.0040	0.06 ± 0.01	0.247 ± 0.002
p-0.007	57.20 ± 1.28	-13221.40 ± 138.44	0.0120 ± 0.0002	1.08 ± 0.02	0.235 ± 0.001
p-0.07	70.76 ± 3.62	-16922.68 ± 159.09	0.0190 ± 0.0009	1.93 ± 0.03	0.232 ± 0.002
f-0.007	79.08 ± 1.92	-20376.10 ± 183.70	0.0408 ± 0.0025	0.24 ± 0.02	0.242 ± 0.003
f-0.07	51.18 ± 6.40	-11878.22 ± 181.50	0.1205 ± 0.0005	0.03 ± 0.001	0.233 ± 0.003

volume data [95], while ASC (adiabatic scanning calorimetry) data gives 0.09 K [28]. Optical measurements [43,47] gives $\Delta T^{**} \approx 0.2$ K on average for the neat 8CB as well. Furthermore, across the N-I transition, some conflicting results have been reported for the same parameters, like the values for ΔT^{**} , in fitting equations, when produced from measurements of different physical properties [2,17,21,42,46,51,52]. Some additional theoretical and experimental studies seem necessary for resolving those kinds of inconsistencies. Given the published values for ΔT^{**} , our reported 0.06-K-value seems to be consistent with them and reasonable to assess the metastable region of the 8CB host as well and hence could be used as a standard reference for further theoretical and experimental studies. As followed from Table III that for all doped (8CB+MWCNT) samples, the average value of the temperature metric ΔT^{**} was found to be 0.82 ± 0.02 K, while this value was reported as 0.67 ± 0.03 K based on $\Delta n(T)$ data previously [37]. One can attribute this difference to the presence of quite small pseudonematic domains in the isotropic liquid phase, quite frequently encountered during dielectric measurements [60,62,63,67]. To date, there exists neither a theory nor an experimental study to enable a link between the value of the temperature metric ΔT^{**} and how the nanosized particles and their interactions depend on the nature of the LC structure. The responses to those issues seem essential for further future studies related to the N-I transition [40,41,52]. At first glance, from Table III, for p-MWCNT-doped samples, the ΔT^{**} values are seen to exhibit a clear trend with p-MWCNT content, while for f-MWCNT samples the values have no such a trend, and additionally, for the f-0.07 sample, the ΔT^{**} is seen to be as small as that of the 8CB host. The shorter-tail LCs are known to exhibit a narrower metastable temperature regime [50]. Thus, it is quite plausible to expect a wider metastable temperature regime, due to the longer alkyl chain of the 8CB LC host, for 8CB+p-MWCNT samples. But for f-MWCNT-doped samples, the surface treatment is known to give rise to well dispersion of MWCNTs in the 8CB host. Thus, this treatment would probably cause the 8CB+f-MWCNT system to act as an effectively shorter-tail system together with an isotropic orientational distribution of f-MWCNTs as compared to p-MWCNT-doped samples. Also, due to the surface treatment, f-MWCNTs could come into play to act like a mesogenic dopant in the 8CB host, resulting in a decrease in ΔT^{**} values. Also, for the 8CB+p-MWCNT composites, there could exist some particular domain structures enforced by the increasing disorder, giving rise to higher

ΔT^{**} values. Additionally, a uniform nematic director field for all MWCNT-doped samples was observed previously [62] via POM, which signals no phase-separate on the macroscopic level. However, the nanoscopic phase separation and diffusion of MWCNT in LC media could still be possible, which might result in this type of ΔT^{**} behavior.

Besides, the critical exponent value (cf. Table III) for the neat 8CB was found to be $\beta = 0.247 \pm 0.002$, the same as the one reported by Thoen and Menu [56]. In addition, the abovementioned computational studies [85,86] discussed the change in the value of the exponent β as a simple indicator of the effects of adding nanomaterials to LCs. In those studies, although the Haller extrapolation [47,50] technique was used, the matter was to present the change in the value of β due to nanomaterials. The authors obtained a 15.6% change in the β exponent with the inclusion of rodlike NPs to the neat LC via simulations [85,86]. In the present $\Delta\varepsilon$ study, together with our previous birefringence Δn study, we claimed a 4% change in the β value due to the addition of MWCNTs. Hence, our result for this change seems more reliable than that given in Refs. [85,86] since our fitting expression has proven to be superior to using the Haller approximation [37,42,43]. There besides, the average value of the exponent β , characterizing the limiting behavior of the nematic order parameter near T_{IN} , was documented as 0.23 ± 0.002 (cf. Table III), which has good consistency with the previously reported value based on $\Delta n(T)$ measurements [37]. Thereby, together with a finite jump in $\Delta\varepsilon$ at T_{IN} (cf. Fig. 1) and considering the margin of the error, the obtained values of the exponent β (cf. Table III) are all around 0.25, which is itself in good accord with TCH [45,57], as was advocated first by Keyes and Anisimov [45,57] and subsequently outlined by many other groups [47,48,51,53,55,96–98]. Although the β values of MWCNT-doped 8CB samples are a bit less than that of the host 8CB, the pretransitional behavior across T_{IN} seem still within the tricritical regime for all doped 8CB samples. In the past, Simeão *et al.* showed that [99–101], by using the experimental data from various anisotropic physical quantities, the behavior of the N phase could exhibit a global universal behavior consistent with TCH, at least in pristine LCs. Given our present results together with those based on high-resolution $\Delta n(T)$ data [37,43], a lack of impact of the MWCNTs on the universal properties of the N-I transition can be concluded. Particularly, experiments based on imposing external fields could allow closer approaches to the possible tricritical regime.

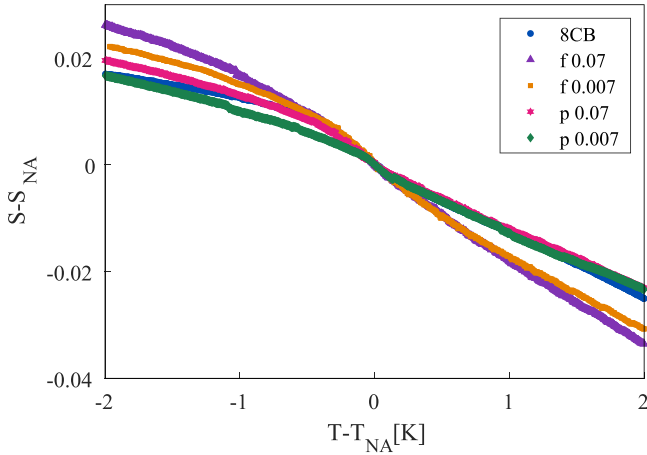


FIG. 2. Detailed plot of $S - S_{NA}$ versus $T - T_{NA}$ in the vicinity of the N-Sm-A transition of all samples over a 4K temperature window of below and above the T_{NA} . Different MWCNT contents χ are indicated in the figure.

C. The nematic-smectic-A transition: The upper limit of the latent heat and the pretransitional anomaly

Turning to the N-Sm-A transition of both the 8CB host and 8CB+MWCNT composites, in this subsection, we present the upper limit of the latent heat ΔH_{NA} , and the behavior of critical fluctuations appearing across the T_{NA} transition temperature. With this regard, we have employed our high-resolution $\Delta\varepsilon(T)$ data and have then compared the so-obtained results with the existing ones in the literature. Of note is that in our previous work [37], the high-resolution optical birefringence $\Delta n(T)$ data have been successfully exploited to investigate the criticality in the vicinity of the N-Sm-A transition, while in the present case, high-resolution $\Delta\varepsilon(T)$ data have just been employed as another physical observable to probe this behavior for the same LC host and 8CB+MWCNT blends as well. As outlined previously, upon further lowering temperature toward T_{NA} , the de Gennes coupling is known to manifest itself by a quite discernible increment in $\Delta\varepsilon(T)$, accordingly in the N order parameter $S(T)$ (cf. Fig. 1). To get an insight regarding the de Gennes coupling strength, sketched in Fig. 2 is the variation of the N order parameter, derived from Eqs. (3) and (5), $S - S_{NA}$ versus $T - T_{NA}$ over a 4K window, just below and above the T_{NA} transition, for all investigated samples. As followed by Fig. 2, a substantial pretransitional effect of the de Gennes coupling is quite apparent above and below T_{NA} . For all investigated samples, we have observed no appreciable thermal hysteresis, signifying that the samples do not phase separated on the macroscopic level, and no apparent discontinuity in our data across T_{NA} within the experimental resolution, which signals the second-order character of the transition qualitatively. The fact that the N-Sm-A transition for both pure 8CB and all 8CB+MWCNT samples remains continuous is in close agreement with the results from our high-resolution optical birefringence $\Delta n(T)$ measurements [37] (cf. Fig. 2 in Ref. [37]). Thus the reported ΔH_{NA} values in this work refer to the possible upper limit of the latent heat of a continuous transition for all samples.

As envisaged by HLM theory, the N-Sm-A transition must be weakly first order. Thus, one should expect a fairly small but measurable discontinuity in the nematic order parameter $S(T)$ at the T_{NA} temperature. Thus, to investigate this issue, the experimental acquisition of high-temperature-resolution $\Delta\varepsilon(T)$ data is merely the first step. The second one is a thoughtful theoretical analysis of the data to determine the ΔH_{NA} values (cf. Eq. (11), also see Ref. [29] for more details). Together with the so-obtained latent heat values, the characterization of pretransitional wings above and below the N-Sm-A transition is also requisite, as will be discussed later. Here, we first focus on the 8CB host and obtain the upper limit of this discontinuity, viz. $\Delta S_{NA}(T_{NA}) = S_A - S_N$, in $S(T)$ across T_{NA} from our $\Delta\varepsilon(T)$ data. Yet, whether $\Delta S_{NA}(T_{NA})$ is exactly zero (at a continuous transition) cannot be experimentally well documented due to the finite resolution. However, all what one can do is to set an upper limit for ΔS_{NA} and accordingly for the latent heat ΔH_{NA} based on the resolution of the experimental data. As was highlighted elsewhere [29], of particular importance would then be the precision in the N order parameter $S(T)$ derived from $\Delta\varepsilon(T)$ [cf. Eq. (5)] as well as the resolution and stability in the temperature readings during the experiment and also the number of experimental data points around the phase transition. Thus, owing to our high-precision and high-temperature resolution $\Delta\varepsilon$ measurements, we have achieved, in this work, the required resolution to extract the upper limit of the latent heat ΔH_{NA} across T_{NA} . Thus, upon a quite attentive inspection of $S(T)$ data (cf. Fig. 2), derived from our $\Delta\varepsilon(T)$ data, in the immediate vicinity of T_{NA} , we have arrived at the upper limit of $\Delta S_{NA} \leq 0.00015$ for the 8CB host in the present work. Then, the corresponding to the reduced entropy difference will then be $\Delta\bar{S}/R = 3.5 \times 10^{-4}$, with R the gas constant, which is in line with adiabatic scanning calorimetry (ASC) measurements [28] and the HLM theory as well [45]. We must emphasize that $\Delta\bar{S}/R$ value reported here is in fairly good agreement with the one obtained via high-resolution $\Delta n(T)$ measurements [29] for the neat 8CB. In our previous work [29], for the neat 8CB, we arrived at the value $\Delta\bar{S}/R = 4.2 \times 10^{-4}$, corresponding $\Delta S_{NA} \leq 0.00020$ based on our high-resolution $\Delta n(T)$ measurements. Based on $\Delta\varepsilon(T)$ data presented here, the corresponding ΔH_{NA} value of the 8CB host is given in Table II. Also, it is worth recalling that the ΔH_{NA} value so-produced from dielectric anisotropy, ASC, and optical birefringence measurements are in line with each other within the experimental uncertainties and this has been shown for the first time in the present work. In the past, although Thoen and Menu presented high-resolution static dielectric permittivity measurements of the 8CB compound [56], yet no value for the upper limit of the latent heat across the N-Sm-A transition was addressed by the authors, so a further comparison is not possible. Hereby, the conclusion drawn here is that the N-Sm-A transition of 8CB is continuous within experimental resolution via calorimetrically [28] and optically [29] and dielectrically together with this work, but consistent with the possibility of very small latent heat expected from the HLM theory.

Motivated by the results of the neat 8CB obtained here, as a further step, for the sake of comparison with the previously published results, in this work, we have also derived the ΔH_{NA} values for the continuous N-Sm-A transition of

8CB+MWCNT nanocomposites from a detailed inspection of $S(T)$ data across T_{NA} . Thereby, the so-produced ΔH_{NA} values of all 8CB-MWCNT composites are presented in Table II. The uncertainty in ΔH_{NA} values obtained by the presented method is about typically 8.5% on average. As followed from Table II, the ΔH_{NA} values of MWCNT-doped samples are higher than that of the 8CB host. One can attribute this apparent increase in ΔH_{NA} values compared to the 8CB host to the that the MWCNT coupling to the LC order could result in some extra energy modes and the smectic fluctuations get modified to some extent due to the presence of MWCNTs [31,32,37]. Of particularly noticing is that the consistency between the two sets of the ΔH_{NA} values produced from $\Delta\varepsilon(T)$ and $\Delta n(T)$ measurements [37] (cf. Table 3 in Ref. [37]) must be regarded as satisfactory, which indicates the robustness of our method to derive those latent heat values. We must emphasize here that ASC is capable of measuring high-resolution temperature variation of both specific heat capacity and enthalpy in the vicinity of the liquid crystalline phase transitions [21]. Thus, since that ASC can discriminate the first-order and continuous phase transitions, and also the effective exponent values can be extracted, apart from high-resolution optical birefringence and dielectric anisotropy measurements ASC results seem essential. At this stage to get an idea about the so-derived ΔH_{NA} value for 8CB+MWCNT system and also for comparison purposes, we refer here to the latent heat values for some LC mixtures derived via ASC. In a recent paper, Thoen and coworkers [102] have presented the latent heat values for the first-order N-Sm-A transition for the 8OCB+9DBT and the 9OCB+9DBT systems (for the meaning of the abbreviation 9DBT see Ref. [102]). The typical values were reported as 435 J/kg for the former and 1300 J/kg for the latter system (see Table 6 and Fig. 9 in Ref. [102]). Similarly, for the 8OCB+9OCB system [24], 400 J/kg (cf. Fig. 8(b) in Ref. [24]) was reported for the first-order N-Sm-A transition as well. Also, it is worth recalling that in the past, with the help of Eq. (11), quite consistent latent heat values for the 8OCB+9OCB system were extracted from our high-resolution $\Delta n(T)$ data by our group as well [26] (see Figs. 6 and 7 in Ref. [26]). As compared to our results for the 8CB+MWCNT system presented here, the abovementioned latent heat values seem nearly two orders of magnitude larger, on average, than ours. For further comparison, we compare our ΔH_{NA} latent heat results of the 8CB+MWCNT system presented here with the latent heat values of the LC mixtures given in Table 6 of Ref. [102], which have the same McMillan ratio R_M as the one of the 8CB+MWCNT system. From the inspection of Table 6 of Ref. [102], the average value of the latent heats for the 8OCB+9DBT and the 9OCB+9DBT systems, for those with average $R_M = 0.973$, is about 33.6 J/kg, while the average value of ΔH_{NA} for the 8CB+MWCNT composites (with average $R_M = 0.971$) is 8.82 J/kg. It is clearly seen that those values are larger by a factor of 4.34 than ours. This comparison confirms that for the 8CB+MWCNT system the N-Sm-A transition is continuous. Additionally, it would be intriguing to make high-resolution ASC measurements for the latent heats for further corroboration of our results. However, it can be claimed that since ASC measurements are absent at this stage to compare with our ΔH_{NA} values, one cannot rule out that the N-Sm-A transition for the

8CB+MWCNT system could be weakly first order in nature. Up to date, for the latent heat ΔH_{NA} values near T_{NA} for various liquid crystalline systems, the excellent agreement has been well documented unambiguously between ASC measurements and high-resolution $\Delta n(T)$ measurements [21,24–26,28,29,43]. Therefore, together with our previous studies, we have just well documented, for the first time, that not only high-resolution optical birefringence $\Delta n(T)$ but also high-resolution dielectric anisotropy $\Delta\varepsilon(T)$ measurements can be employed to derive the latent heat values in the vicinity of the N-Sm-A transition of liquid crystalline systems. In the past, in a paper by Sigdel and Iannacchione [36] the fluctuation induced pretransitional enthalpy δH_{NA} values, being an integral of the excess specific heat capacity at a fixed probing frequency [19,30], of some 8CB-p-MWCNT composites were presented. The authors argued that the N-Sm-A transition remains continuous for all composites studied and their δH_{NA} values increased as compared to that of the 8CB host as well. Despite the meanings of ΔH_{NA} and δH_{NA} being slightly different, their trend with MWCNT content seems the same.

In our earlier studies [25,29,37,43], high-resolution $\Delta n(T)$ data has been successfully exploited to explore the critical behavior in vicinity of the N-Sm-A phase transition of various liquid crystalline systems. In the present case, we now utilize our high-resolution $\Delta\varepsilon(T)$ measurements to perform the critical exponent analysis for 8CB+MWCNT blends near the N-Sm-A phase transition. As seen from Fig. 2, a strong thermal variation of the N order parameter around T_{NA} , i.e., a pronounced pretransitional behavior, which gives rise to an enhancement of $S(T)$ in the Sm-A phase is quite apparent. This is quite similar to the case seen in the $\Delta n(T)$ measurements [37]. Moreover, in liquid crystalline compounds exhibiting the N-Sm-A phase sequence, the occurrence of the smectic layering causes the orientational ordering to enhance [20,45]. Based on rather general consequences of the Landau-de Gennes free energy [1,45,103] one can derive (see below) the following expression for the temperature variation of Ψ^2 :

$$\Psi^2 = L + M_{\pm}|t|^{1-\alpha}, \quad (12)$$

where $t = (T - T_{NA})/T_{NA}$ is the reduced temperature difference, T_{NA} is the N-Sm-A transition temperature, and α is the specific heat capacity exponent. Here and hereafter, the signs (+) and (−) stand for, respectively, data above and below T_{NA} , respectively. It is quite well known that the N-Sm-A transition is fluctuation dominated, and one can estimate the effect of those fluctuations on the N order parameter by assuming a proportionality between the enhancement in the N order parameter as δS and the entropy change $\Delta\bar{S}$ [2]. Thus, below, we present the quite general argument predicting Eq. (12) via the Landau-de Gennes free energy. The argument simply starts with the free energy $F = \int d^3r[at\Psi^2 + \delta F(\Psi)]$, and then, calculating the partition function with the help of $Z = \int d\Psi \exp(-F/k_B T)$ with k_B the Boltzmann constant. Differentiation with respect to temperature will yield the excess entropy as $\Delta\bar{S} \sim \Psi^2$. Then, by taking the integral of the singular part of the specific heat capacity, $C_P \sim t^{-\alpha}$, $\Delta\bar{S}$ can be obtained as $\Delta\bar{S} \sim \Psi^2 \sim t^{1-\alpha}$. Also due to $\delta S = c_A \chi_N \Psi^2$ one can reach that $\delta S \sim \Psi^2 \sim t^{1-\alpha}$. We notice here that the validation of Eq. (12) has recently been well established for several types of liquid crystalline systems via high-resolution

$\Delta n(T)$ measurements by our group [25,26,37,42,43] and also by many others [47,69,96,97,104]. But, the usage and the validation of Eq. (12) via high-resolution dielectric anisotropy data are quite interestingly limited [53,54]. Toward this end, we show in the present work that high-resolution $\Delta\varepsilon(T)$ data have convincingly been applied for the critical exponent analysis at the N-Sm-A transition.

In the following part of this subsection the critical exponent analysis for both the neat 8CB and 8CB+MWCNT blends are presented and a comparison with the results obtained by high-resolution $\Delta n(T)$ measurements is discussed. The second-order, viz. continuous, phase transitions are well known to be characterized by the fluctuations in the vicinity of the phase transition point, which diverge in size to infinity for a properly defined order parameter [105]. A power law with a characteristic critical exponent depending on the universality class of the related phase transition could well describe this aforementioned size divergence. An appropriate way to look in great detail at the limiting behavior of the N order parameter near the T_{NA} transition point can be to use both quantities $S(T)$ or $\Delta\varepsilon(T)$. But, we prefer here using our $\Delta\varepsilon(T)$ data directly instead of $S(T)$ to avoid extra errors arising from a nonlinear multi-parameter fitting procedure. As an attempt to get the critical exponent α , one can use the following fitting expression, being reminiscent of the fitting expression for analyzing molar volume data in the literature [106,107]:

$$\Delta\varepsilon(T) = A'_{\pm}|t|^{1-\alpha} + B'_{\pm}|t| + C'_{\pm}. \quad (13)$$

However, to avoid the regular background contribution, resulting from the regular temperature dependence of the N order parameter, one can alternatively fit $\Delta\varepsilon(T) - \Delta\varepsilon_{\text{fit}}(T)$ data to the following form:

$$\Delta\varepsilon(T) - \Delta\varepsilon_{\text{fit}}(T) = A^{\pm}|t|^{1-\alpha} + B^{\pm}|t| + C^{\pm}. \quad (14)$$

In the past, quite similar expressions were successfully applied to quantify the optical birefringence data across the N-Sm-A transition [42] (see Eqs. (13) and (14) in Ref. [42]). Besides, in a paper by Rzoska *et al.* [52], the implementation of the derivative-based analysis is shown to be more useful for critical exponent analysis. Thus, to reveal the pretransitional anomaly more clearly and also to decrease the number fitting parameters, the derivative analysis was performed here. Therefore, given the continuous (second-order) character of the N-Sm-A transition of all samples studied here, to quantitatively characterize the pretransitional anomaly near T_{NA} , one can fit the local slope $D_{\varepsilon} = -d(\Delta\varepsilon)/dT$ according to the simple power-law expression given below, which is itself also consistent with Eq. (12):

$$D_{\varepsilon}(T) = -\frac{d(\Delta\varepsilon)}{dT} = A_{\pm}|t|^{-\alpha} + B, \quad (15)$$

where A_{\pm} are the critical amplitudes and B is the background term. However, it is well known that the local slope $D_{\varepsilon} = -d(\Delta\varepsilon)/dT$ will be significantly too scattered, due to the fairly small temperature difference between the successive data points [25,26,37,42,43,69]. Instead, a further reduction in scatter has been asserted to be possible by defining a differential quotient $Q_{\varepsilon}(T)$, given as the following form

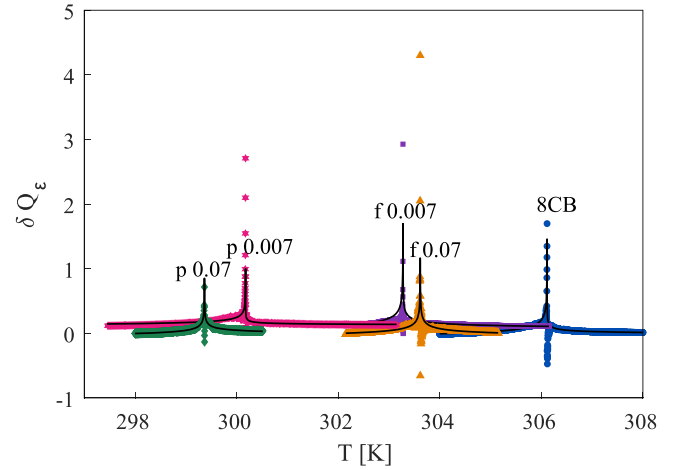


FIG. 3. Overview of the temperature variation of the excess quotient $\delta Q_{\varepsilon}(T)$ in the vicinity of the N-Sm-A transition for 8CB+MWCNT composites together with the 8CB host. The solid lines represent the fits to Eq. (17). Different MWCNT weight fractions χ are indicated in the figure. Recall that p and f refer to pristine and functionalized MWCNTs, respectively.

[25,29,37,53,54]:

$$Q_{\varepsilon}(T) = -\frac{\Delta\varepsilon(T) - \Delta\varepsilon(T_{NA})}{T - T_{NA}}. \quad (16)$$

One can easily infer that the differential quotient $Q_{\varepsilon}(T)$ diverges at T_{NA} with the same critical exponent α and the background term as $D_{\varepsilon}(T)$ but for the former with the leading critical amplitude modified by a factor of $(1 - \alpha)^{-1}$. We must emphasize here that the advantage of using the differential quotient $Q_{\varepsilon}(T)$ resides in that it takes into account the chord not the local derivative and is hence less sensitive to noise than $D_{\varepsilon}(T)$. This technique has successfully been used to quantify ASC data [17,21,24] and as well as, very recently, high-resolution optical birefringence $\Delta n(T)$ data [25,26,29,37,42,43,47]. Moreover, the pretransitional anomaly at T_{NA} can be revealed more clearly by subtracting an appropriate background contribution $Q_{\varepsilon}^{\text{bg}}(T)$ from $Q_{\varepsilon}(T)$ [42,43]. This contribution can be evaluated via $Q_{\varepsilon}^{\text{bg}}(T) = -[\Delta\varepsilon_{\text{fit}}(T) - \Delta\varepsilon_{\text{fit}}(T_{NA})]/(T - T_{NA})$. In this manner, one can reveal the critical anomaly more distinguishably in the so-called excess quotient $\delta Q_{\varepsilon}(T) = Q_{\varepsilon}(T) - Q_{\varepsilon}^{\text{bg}}(T)$ across T_{NA} . Displayed in Fig. 3 is the evolution of the excess quotient $\delta Q_{\varepsilon}(T)$ for all 8CB-MWCNT composites together with the 8CB host. As is apparent from Fig. 3, in the vicinity of the T_{NA} , all $\delta Q_{\varepsilon}(T)$ curves exhibit a quite sharp and prominent N-Sm-A transition peak for all samples. On either side of the N-Sm-A transition, no broad tails in the temperature variation of $\delta Q_{\varepsilon}(T)$ curves were also detected. Also, for the p-0.007 and f-0.007 samples, the peak height values of excess quotient $\delta Q_{\varepsilon}(T)$ near T_{NA} are noticed to be a bit higher than those of the other samples including the neat 8CB. Moreover, as may be inferred from Fig. 3, the δQ_{ε} wings are noticed to be quite similar and nearly overlap for all 8CB+MWCNT samples and the 8CB host on both low and high-temperature sides of the N-Sm-A transition, in spite of considerable shifts in the T_{NA} transition temperatures. Furthermore, it is imperative to recall

TABLE IV. Fitting parameter values for the least-squares fit of the excess quotient $\delta Q_\varepsilon(T)$ data with Eq. (17) in the vicinity of the N-Sm-A transition of 8CB+MWCNT composites and the 8CB host. Refer to Table I for the meaning of the abbreviations seen in the first column.

Sample	Phase	α	A'_+ or A'_-	B'
8CB host	N	0.3206 ± 0.0070	0.0102 ± 0.0007	-0.0912 ± 0.0003
	Sm-A	0.3206 ± 0.0080	0.0093 ± 0.0013	
p-0.007	N	0.3202 ± 0.0026	0.0097 ± 0.0007	-0.0269 ± 0.0005
	Sm-A	0.3202 ± 0.0025	0.0162 ± 0.0003	
p-0.07	N	0.3212 ± 0.0090	0.0135 ± 0.0004	-0.0628 ± 0.0005
	Sm-A	0.3212 ± 0.0035	0.0164 ± 0.0003	
f-0.007	N	0.3218 ± 0.0021	0.0189 ± 0.0002	-0.0855 ± 0.0007
	Sm-A	0.3217 ± 0.0015	0.0301 ± 0.0003	
f-0.07	N	0.3208 ± 0.0018	0.0214 ± 0.0002	-0.0659 ± 0.0003
	Sm-A	0.3208 ± 0.0020	0.0223 ± 0.0003	

that in the δQ_ε peaks across the N-Sm-A transition for all MWCNT-doped samples, we have not observed any smeared-out behavior, which is contrary to those seen in the specific heat capacity peaks of 8CB+aerosil and 8CB+aerogel dispersions [19,108,109]. Thus, here one can conclude that in all 8CB+MWCNT composites the bulklike nematic and smectic fluctuations are essentially present and are constant for all samples. The fact that thermal fluctuations remain bulklike indicates no loss in the quasilong smectic order in the 8CB host due to the incorporation of MWCNTs. This is in excellent accord with the results obtained from high-resolution $\Delta n(T)$ measurements [37] and high-resolution a.c. calorimetry data [36] as well. Thus, turning to the critical exponent analysis, instead of using Eq. (15) as argued above, we performed the exponent analysis of our $\delta Q_\varepsilon(T)$ data (cf. Fig. 3) with the help of the following expression:

$$\delta Q_\varepsilon = A'_\pm |t|^{-\alpha} + B', \quad (17)$$

where A'_\pm , B' , and α are free fitting parameters. Also, it can be easily obtained that $B' = B$ and $A'_\pm = A_\pm/(1 - \alpha)$. Above and below T_{NA} , we have carried out simultaneous fits to excess quotient $\delta Q_\varepsilon(T)$ via Eq. (17). For the fitting procedure, we have used a nonlinear multi-parameter fitting program whose details were argued in the preceding subsection, with that the N-Sm-A transition temperature T_{NA} values were held fixed at the values given in Table II. Also, during the fitting procedure, we excluded some data points very close to the T_{NA} to minimize the error resulting from the experimental uncertainty and to realize consistent fitting. We assessed the quality of the fits by evaluating the reduced error function χ^2_v on either side of the T_{NA} , and also tested their stability by employing a double-range shrinking method [93,94]. While evaluating the χ^2_v function, the variance has been obtained from the scatter in the data points. Since the inclusion of the correction terms like $D_\pm |t|^{0.5}$ above and below T_{NA} in Eq. (17) did not improve the fit quality appreciably, one can thus conclude that $\delta Q_\varepsilon(T)$ data are well portrayed by Eq. (17) for all investigated samples. The fits to Eq. (17) are presented as solid lines in Fig. 3 while the least-squares fitting results are gathered in Table IV. As is followed by Table IV, for all investigated samples, the value of the effective critical exponent α is the same for either side of the N-Sm-A transition, within the experimental uncertainty. Besides, one can notice that for all MWCNT-doped samples the variation of the amplitude ratio

A'_-/A'_+ remains nearly the same within the statistical uncertainties and seems to be independent of MWCNT content and surface functionalization of MWCNTs as well. Additionally, its average has been found to be nearly equal to unity, indicating the symmetry of the $\delta Q_\varepsilon(T)$ wings on either side of T_{NA} . However, the value of this ratio for the neat 8CB has been found to be less than those for doped samples, which is also itself consistent with the literature values [21,28,37,103]. Thus, the MWCNT (p-MWCNT or f-MWCNT) doping could be advocated to contribute to liquid crystalline ordering in addition to the 8CB host to some extent, at least locally in the close vicinity of T_{NA} transition temperature. But however, one can remark that the de Gennes coupling also seems not to differ from that of the neat 8CB, due to the fact that the value of the Mac Millan ratio $R_M = T_{NA}/T_{NI}$, the ratio of the temperatures (in K) of the N-Sm-A and N-I, is nearly the same for all samples (cf. Table II). Moreover, we could emphasize that the effective exponent α values and also the behavior of the amplitude ratio A'_-/A'_+ for all samples studied here are in excellent agreement with those extracted from high-resolution optical birefringence measurements $\Delta n(T)$, within the statistical uncertainties (cf. Table 5 in Ref. [37]). As was pointed out above, apart from the quotients $Q_\varepsilon(T)$ and $\delta Q_\varepsilon(T)$, the local slope $D_\varepsilon(T)$ itself can be employed to study the pretransitional anomaly at T_{NA} . In the recent past, a quite similar local slope viz. $D_n(T) = -d(\Delta n)/dT$ extracted from the optical birefringence data was successfully used for various liquid crystalline materials [25,26,29].

Except those, as was outlined in our previous studies, which are applied for the optical birefringence data successfully to date [37,43], in the close vicinity of a continuous N-Sm-A transition, for the sake of simplicity, a much more attractive way is possible for the critical exponent analysis. This can be achieved by combining Eqs. (15) and (17) and also by keeping in mind the relation $A'_\pm = A_\pm/(1 - \alpha)$. Thus, with a quite straightforward calculation, one can obtain the following fitting expression:

$$Q_\varepsilon - D_\varepsilon = \frac{\alpha A_\pm}{1 - \alpha} |t|^{-\alpha}. \quad (18)$$

We stress that this simple method presents a great advantage to eliminate the regular background parameter B [cf. Eqs. (15) and (17)] and, hence, to use also the double-logarithmic form of Eq. (18) in determining the critical

exponent α via a linear regression procedure. Taking the logarithm of both sides of Eq. (18) gives

$$\log_{10}(Q_\varepsilon - D_\varepsilon) = \log_{10}\left(\frac{\alpha A_\pm}{1 - \alpha}\right) - \alpha \log_{10}|t|. \quad (19)$$

As a result, one can obtain a straight line with a negative slope, immediately yielding the critical exponent α itself. We stress that a quite similar technique has been skillfully employed to extract the exponent α from $(C_{\text{cal}} - C_p)$ versus $|t|$ data obtained by ASC [21,24,28,33,110] as well as from $(Q_n - D_n)$ versus $|t|$ data obtained by the optical birefringence Δn measurements [37,42]. To the best of our knowledge, in this work, the usage of Eq. (19) has been presented for the first time for high-resolution dielectric anisotropy $\Delta\varepsilon(T)$ data. This simple method opens an appealing way to determine the critical exponent α across a continuous N-Sm-A transition. It is worth recalling that this procedure is applicable only to second-order transitions, but for weakly first-order transitions separate analyses of the data below and above the transition are necessary. One can do it by allowing T_{NA} and $\Delta\varepsilon(T_{NA})$ in Eq. (16) to be adjustable parameters during the fitting procedure, being different for data below and above the transition. This is quite analogous to the upper stability limit of the nematic phase and the lower stability limit of the isotropic liquid phase for the weakly first-order N-I transition. This approach seems to be applicable for some LC binary mixtures exhibiting the HLM effect [24,25,26] by excluding the data in the two-phase co-existence region. Displayed in Fig. 4 are the plots of $(Q_\varepsilon - D_\varepsilon)$ versus $|t|$ data on a \log_{10} - \log_{10} form for all investigated samples, including the 8CB host, on either side of T_{NA} . Of note is that by using Eq. (19) one can derive from the negative slope of a \log_{10} - \log_{10} plot (cf. Fig. 4) $(Q_\varepsilon - D_\varepsilon)$ versus $|t|$ data on either side of T_{NA} to produce the (effective) critical exponent α values. Toward this end, we have separately fitted both wings of the N-Sm-A transition to Eq. (19) to produce those α values. Also, that quite similar α values were extracted above and below T_{NA} must here be stressed. The values of the effective critical exponent α (average value from below and above T_{NA}) for both 8CB and 8CB+MWCNT blends are presented in Table II. It is worth recalling that we take the uncertainty in α as the difference between the α values above and below T_{NA} (cf. Table II) [30,111]. Additionally, we have also calculated the average limiting slope of the data presented in Fig. 4 for each sample over the reduced temperature range approximately $\log_{10}|t| < 2.5$. Then, we have found that the estimated value of the slope of the solid line given in Fig. 4 is in excellent consistency with the values given in Table II for each sample. One can notice that there exists noisy behavior in the N wings compared to the Sm-A wings away from the N-Sm-A transition for all samples as seen in Fig. 4. That the fluctuations of the high-temperature phase, namely in the isotropic liquid phase, would probably give rise to some additional noise in the \log_{10} - \log_{10} curves could be the reason for this behavior, which does not affect the critical exponent values substantially. However, similar noisy behavior in the N wing away from T_{NA} is also observed both in $\log_{10}(C_{\text{cal}} - C_p)$

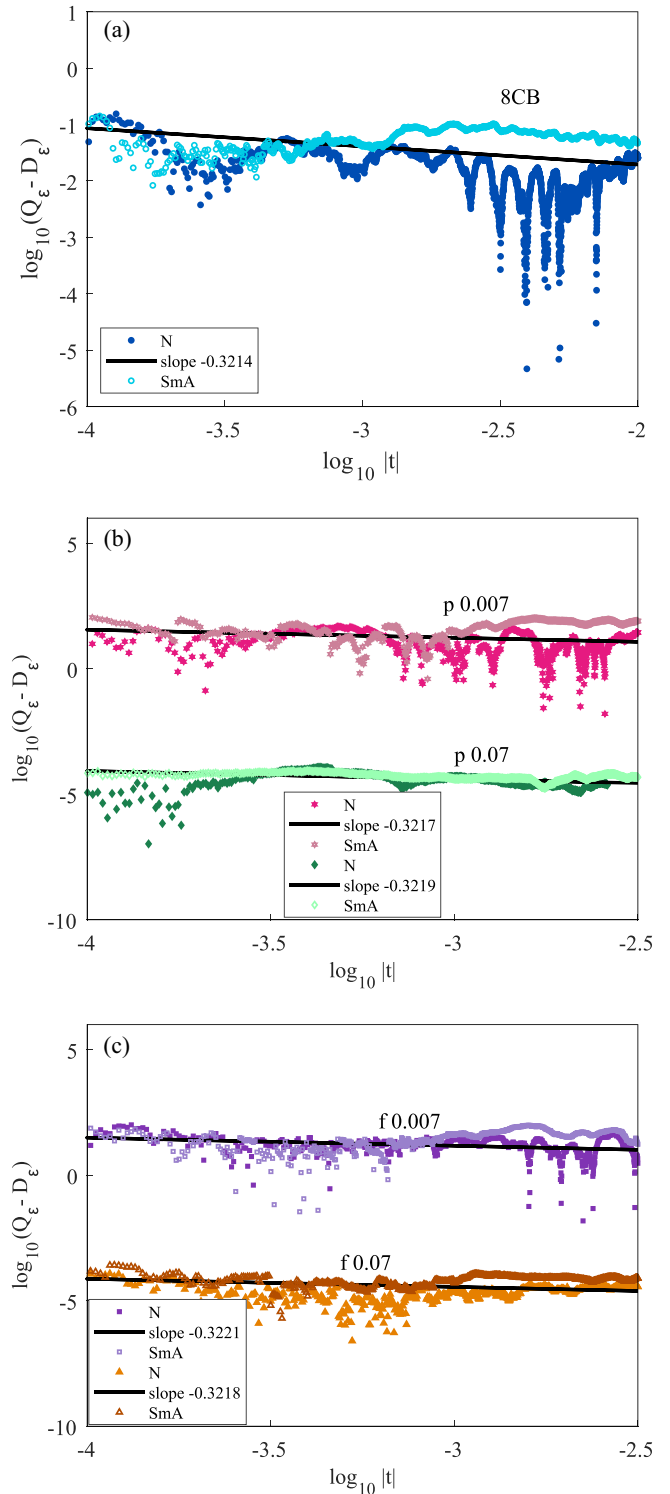


FIG. 4. The \log_{10} - \log_{10} plot of the difference $(Q_\varepsilon - D_\varepsilon)$ as a function of the reduced temperature difference $|t|$ yielding the effective critical exponent α values in the close vicinity of the N-Sm-A transition T_{NA} for (a) the 8CB host, (b) 8CB-p-MWCNT, and (c) 8CB-f-MWCNT composites. Recall that the average limiting slope of the solid line in each figure is consistent with the values given in Table II for each sample.

versus $\log_{10}|t|$ curves produced from ASC data [21,24,102] and $\log_{10}(Q_n - D_n)$ versus $\log_{10}|t|$ curves obtained from optical birefringence data by our group [37]. Since a similar type of noise is seen in all log-log curves produced from ASC, Δn , and $\Delta \varepsilon$ data, this might be due to the first-order character of the N-I transition which directly affects the numerical differentiation (cf. $D_\varepsilon = -d(\Delta \varepsilon)/dT$, $D_n = -d(\Delta n)/dT$ [37], $C_p = P/(dT/dt)$ for ASC data [21,24,102]). In addition, by examining the gap between two slope lines of the linear fit of our \log_{10} - \log_{10} plots of $(Q_\varepsilon - D_\varepsilon)$ versus $|t|$ data (cf. Fig. 4), we have extracted a qualitative measurement of the critical amplitude ratio A_-/A_+ . Besides, from those A_\pm values, we have obtained that $A'_+/A_+ \approx A'_-/A_- \approx 1.48$. Especially note the fact that this finding is fully in line with the relation $A'_\pm = A_\pm/(1 - \alpha)$ for the reported α values. As may be seen from Tables II and IV, the values of the effective critical exponent α of 8CB+MWCNT blends seem to be the same as that of the 8CB host within the statistical uncertainties, which thoroughly confirms the nematic and smectic fluctuations for 8CB+MWCNT blends resembles essentially bulklike, being independent of the surface functionalization of MWCNT dopants. Furthermore, we stress here that the obtained results for the neat 8CB via $\Delta \varepsilon(T)$ data are fully consistent with the anisotropic correlation lengths, based on x-ray measurements [17,21] within the framework of a hyperscaling relation [45,105]. Also, particularly recall that our findings in the present work are in full accord with the ones based on high-resolution optical birefringence measurements [37]. Besides, a quite similar behavior for the N-Sm-A transition has recently been well documented in 8CB+CdSe mixtures based on the optical birefringence data [43]. Given the extracted values of the exponent α for both the neat 8CB and 8CB+MWCNT blends, the effective critical exponents lie in between tricritical (TCP) value $\alpha_{TCP} = 0.5$ and the 3D-XY value of $\alpha_{XY} = -0.01$ because of the observed rather narrow NR's and also, the coupling between the N and Sm-A order parameters for all samples. Liquid crystalline materials with small NR are known to have small splay elastic constant K_{11} values at the transition point T_{NA} [1]. With the inclusion of MWCNTs in the neat 8CB, although there exists an enhancement in NR values to some extent (cf. Table II), their K_{11} values at T_{NA} do not follow the same increment trends [62,63]. As discussed elsewhere [62], this may be due to the Berreman and Meiboom conjecture [112] which claims that for MWCNT-doped samples elastic interactions will result in higher-order deviations from the mean-field behavior $K_{11} \propto S^2$. By taking into account the high aspect ratio of MWCNTs together with the longer alkyl chain of the 8CB LC host, the reported deviations from $K_{11} \propto S^2$ data seems quite rather reasonable. Additionally, it is quite well-known that de Gennes coupling (cf. $\delta S = C_A \chi_N \Psi^2$) reveals the effects of elasticity of the nematic ordering prior to the onset of the smectic order [1,2]. Also recall that the increase in the NR values with MWCNT doping signals a decrease in the nematic susceptibility χ_N , causing the director fluctuations to suppress. However, by taking into account that for MWCNT-doped samples the critical exponent α values and the McMillan ratio R_M values are nearly the same as that of the 8CB host, the combined effect of $C_A \chi_N$ is not strong enough to cause the disorder-driven decoupling between the N and Sm-A order parameters,

thus not making the N-Sm-A transition more continuous. This behavior can be ascribed to the weaker nature of MWCNT disorder. Thus, one can infer that the pinning of LC molecules at the surface of MWCNTs and elastic coupling cannot result in a turning-off of the de Gennes coupling and the $\delta \hat{n} - \Psi^2$ coupling playing no important role across the N-Sm-A transition. For 8CB+MWCNT system, the N-Sm-A transition is still away from the 3D-XY fixed point. We must emphasize that this observed behavior in 8CB+MWCNT systems is also remarkably different from the ones observed in 8CB+aerosil and also 8CB+aerogel systems [19,108,109]. In those types of systems, the inclusion of aerosil and aerogel NPs was documented to destroy the transition to a quasi-long-range-ordered smectic phase and replace it with the formation of short-range correlations [108,109]. The nature of the N-Sm-A transition for those systems was observed to approach the 3D-XY fixed point, which would be expected in the absence of both de Gennes and $\delta \hat{n} - \Psi^2$ couplings, with aerosil and aerogel loading and to exhibit downward shifts in the phase transition temperatures. Thus, one can infer that the effect of MWCNTs on the N-Sm-A transition of the 8CB host seems to resemble the so-called floppy regime, as was documented at low contents of LC+aerosils dispersions can be advocated [19,43].

In a recent study, Kalakonda *et al.* [113] presented a comparative study on the impact of MWCNT doping on the phase transition behaviors of both 8CB and $\bar{9}.O.4$ (4-butyloxyphenyl-4'-nonyloxybenzoate) LC hosts. They claimed that the interactions between MWCNTs and the host LC are quite different for 8CB and $\bar{9}.O.4$. Moreover, it is quite well-known that nCB and also nOCB homologs exhibit strong antiparallel coupling between the large terminal dipoles, giving rise to a so-called incommensurate partial bilayer smectic- A_d (Sm A_d) with d around 1.5 times the molecular length [20,42]. It would also be quite intriguing to investigate whether high-resolution dielectric anisotropy $\Delta \varepsilon(T)$ data could be exploited to reveal the latent heats and the effective critical exponents at T_{NA} for LC materials, exhibiting a normal monolayer smectic phase (Sm A_m) such as nonpolar $\bar{n}.O.\bar{m}$ (4-alkyloxyphenyl-4'-alkyloxybenzoate) homologs [42], since the fact that the magnitude of the enhancement δS of the N order parameter is smaller for LCs with the Sm A_d phase than those with Sm A_m phase for a given value of the McMillan ratio R_M [20,42] is well-documented.

V. CONCLUDING REMARKS

In this work, we present rigorous high-temperature resolution and highly precise experimental data for the temperature dependence of the dielectric anisotropy for the 8CB host and the 8CB+MWCNT blends over the temperature range for which the N-I and N-Sm-A phase transitions take place. The dielectric anisotropy $\Delta \varepsilon(T)$ data have then been utilized to probe the temperature variation of the N order parameter across both the N-I and the N-Sm-A phase transitions of all investigated samples. We have observed that the T_N and T_{NA} phase transition temperatures of the 8CB+MWCNT system shift downwards with the inclusion of both types of MWCNTs to the 8CB host by indicating a nonlinear χ dependence. From the observed suppression of the transition temperatures,

a CNT-induced disorder seems to play a predominant role is noted. One can claim that since the local ordering of MWCNTs is randomly arranged, leading to a random-field effect, an overall disordering of the samples is observed. Additionally, the larger T_{IN} and T_{NA} downward shifts seen in p-MWCNT-doped samples could be attributed to the fact that the surface ordering tendencies seem larger in f-MWCNT-doped samples, while the elastic distortions are comparable for both types of MWCNT dopants. It is worth noting that this type of temperature behavior has also been observed [19,114,115] in mixtures of different LCs and aerosil NPs. For the 8CB+p-MWCNT system, the nematic temperature range NR increases at a higher rate as compared to the 8CB+f-WCNT system. These differences might be due to the surface treatment of the latter. But, on average, a nearly 20% change seen in NR for the 8CB+MWCNT system could be attributed to the stabilization of the N phase, as compared to the 8CB host. Although the inclusion of MWCNTs in the 8CB host manifests itself as a random dilution effect, it is worth noting that the phase transition characteristics remain bulklike. A recent investigation performed on the nOCB+SWCNT system [116] asserted that mesophase stabilization can be explained by the nanophase segregation model [117]. Thus, the fact that the difference in the aspect ratio of the LC host and SWCNT might cause this segregation has been emphasized. It would be intriguing to investigate whether this presented model applies to our case because both nCB and nOCB homologs exhibit the same type of mesophases with a large dipole moment of the terminal -CN group, oriented along the long molecular axis. We also briefly discussed a possible relevant phenomenological theory concerning the so-observed depression in the transition temperatures [73–75]. One can also advocate that based on the Berreman and Meiboom conjecture, in the aforementioned theory the inclusion of some elastic interaction terms cannot be ruled out. Besides, in some investigations, the principal parameter governing the coupling between CNTs and LCs is proportional to the diameter of CNTs was reported [75,76]. Thus, for the forthcoming studies in future recent, it would be more intriguing to investigate the phase transition behavior and its criticality of the LC+CNT system as a function of the MWCNT size, namely diameter, instead of the content. Hence, it could be possible to investigate whether the shifts in the transition temperatures ΔT_{IN} and ΔT_{NA} exhibit a power-law dependence with the diameter, as was previously reported for some 8CB-hosted systems [73].

For both investigated p-MWCNT and f-MWCNT contents in 8CB+MWCNT blends, it has been well documented, from our precise $\Delta\varepsilon(T)$ data, that the N-I transition is clearly identified as weakly first order in nature while the N-Sm-A transition remains continuous for all MWCNT contents regardless of the surface functionalization of MWCNTs. In so-far, the N-I transition has frequently been investigated via dielectric permittivity data, based on “the so-called fluidlike model” for several nCB, nOCB homologs, [40,41,50–55], whereas in this work, for the first time, the related critical exponents and also the temperature metric of the discontinuity of the N-I transition have been determined from the order parameter $S(T)$ within the framework of the Maier-Meier theory [cf. Eq. (5)]. A particular emphasis has also been devoted to the N-Sm-A phase transition, and with this regard, we have

extracted the upper limits for the latent heat ΔH_{NA} , which is itself related to the upper bound in the discontinuity, for both the 8CB LC host and all 8CB+MWCNT blends via a detailed inspection of the behavior of the N order parameter in the close vicinity of T_{NA} . For the first time, upon close examination of $S(T)$ data, derived from our high-resolution $\Delta\varepsilon(T)$ measurements, in the vicinity of T_{NA} , we have arrived at the upper limit of the latent heat ΔH_{NA} as 3.03 J/kg for the 8CB host. It must be stressed that this yielded latent heat value for the 8CB host is in fairly good agreement with the one produced previously via high-resolution optical birefringence $\Delta n(T)$ measurements by us [29] and with ASC measurements [28] as well. Motivated by this result, then, the ΔH_{NA} values of 8CB+MWCNT blends were also derived and were found to be higher than that of the 8CB host, which is in line with those produced via high-resolution optical birefringence data [29,37]. Moreover, by exploiting the fact that the temperature gradient of the N order parameter across T_{NA} exhibits the same power-law divergence as the specific heat capacity, a thorough critical exponent α analysis has been performed via several fitting expressions [cf. Eqs. (17) and (19)], and the so-obtained α values of all 8CB+MWCNT blends, regardless of the surface functionalization, are observed to be comparable to that of the 8CB host within the experimental uncertainty. We remark here that for the neat 8CB, the produced α values are in excellent agreement with those obtained from the high-resolution optical birefringence measurements by us [29,37] and ASC measurements [28]. Hence, like the differential quotient $Q_n(T)$ (cf. Eq. (11) in Ref. [37]), the differential quotient $Q_\varepsilon(T)$ is shown to be sensitive to the Sm-A ordering and can thus be used to probe the critical behavior across T_{NA} . While this issue has been addressed previously by the others [53,54], for the first time, we have tested, in this work, the validation of Eq. (19) for producing the critical exponent α values by the usage of both the local slope $D_\varepsilon(T)$ and the differential quotient $Q_\varepsilon(T)$ data, thus which itself leaves out any background term from the fitting procedure. We have concluded that the presence of MWCNTs in 8CB seems as introducing a weak-strength random field that is not enough to compete with smectic ordering in the host LC, which is contrary to the case of 8CB+aerosil and 8CB+aerogel systems. It is imperative to note that disordering character is not strong enough to derive a decoupling between the N and Sm-A order parameters. The critical behavior of the 8CB+MWCNT system has been shown to be dominated by a crossover from the 3D-XY to tricritical. To the best of our knowledge, for the first time in this work, we have shown that high-resolution dielectric anisotropy $\Delta\varepsilon(T)$ data is as adequate as both calorimetric and high-resolution optical birefringence $\Delta n(T)$ data to determine the nature of the N-Sm-A transition and as well as to extract the upper limit of the associated latent heat value. It is worth recalling here that apart from high-resolution optical birefringence and dielectric anisotropy measurements, ASC results seem essential since being capable of discriminating the first-order and continuous phase transitions.

To get more insight into the impact of MWCNTs on the phase transition characteristics of the neat 8CB, thermal transport parameters such as the thermal diffusivity and the thermal conductivity measurements, based on the photopyroelectric

technique [2,118], would be quite advantageous. Also, continued experimental attempts seem to be needed, especially x-ray or neutron scattering studies, which probe directly the smectic correlation function [109]. One challenge for future can be to explore the the connection between anisotropic ξ_{\parallel} and ξ_{\perp} behavior, where ξ_{\parallel} and ξ_{\perp} are the correlation lengths parallel and perpendicular to the normal to the smectic layers, and pseudoisotropic $\xi_{\parallel}\xi_{\perp}^2$ behavior via two-scale universality and to compare them with those obtained from x-ray measurements directly.

Additionally, in a more recent, the test of the HLM crossover function at T_{NA} in some LC binary mixtures was presented via high-resolution Δn measurements by our group [25,26] and we obtained a fairly good agreement with the existing results based on ASC measurements [24]. Hence, it seems intriguing to investigate whether the high-resolution dielectric anisotropy $\Delta\epsilon(T)$ data can be utilized to verify the HLM effect for some binary LC mixtures as was done previously via Δn data. It is our opinion that those findings based

on our approach presented here [cf. Eqs. (11) and (19)] could pave the way for further studies aiming at determining the nature of the N-Sm-A transition for several types of LC-based nanocomposites.

ACKNOWLEDGMENTS

This work was supported by the Research Fund of Istanbul Technical University under Grant No. 40883. We cordially thank BAYER (Germany) for providing us with free samples of both pristine and -COOH functionalized MWNCTs. We appreciate Dr. Selma Ergin, Faculty of Naval Architecture and Ocean Engineering-Ship Emissions Laboratory, for the usage of Ultra-Micro Balance during the preparation both 8CB-p-MWCNT and 8CB-f-MWCNT samples. The authors declare that they have no known competing financial interests or personal relationships that could have appeared to influence the work reported in this paper.

-
- [1] P. G. de Gennes and J. Prost, *The Physics of Liquid Crystals*, 2nd ed. (Oxford University Press, Oxford, UK, 1993).
- [2] M. Marinelli, F. Mercuri, and U. Zammit, in *Heat Capacities: Liquids, Solutions, and Vapours*, edited by E. Wilhelm and T. M. Letcher (Royal Society of Chemistry, London, UK, 2010), p. 367, and references cited therein.
- [3] O. Stamatiou, J. Mirzaei, X. Feng, and T. Hegmann, *Top. Curr. Chem.* **318**, 331 (2012).
- [4] Y. Garbovskiy and I. Glushchenko, *Crystals* **5**, 501 (2015).
- [5] M. Urbanski and J. P. F. Lagerwall, *J. Mater. Chem. C* **4**, 3485 (2016).
- [6] S. Pandey, D. P. Singh, K. Agrahari, A. Srivastava, M. Czerwinski, S. Kumar, and R. Manohar, *J. Mol. Liq.* **237**, 71 (2017).
- [7] P. Tripathi, M. Mishra, S. Kumar, R. Dabrowski, and R. Dhar, *J. Mol. Liq.* **268**, 403 (2018).
- [8] Khushboo, P. Sharma, P. Malik, and K. K. Raina, *Liq. Cryst.* **44**, 1717 (2017).
- [9] B. Liu, Y. Ma, D. Zhao, L. Xu, F. Liu, W. Zhou, and L. Guo, *Nano Res.* **10**, 618 (2017).
- [10] I. Dierking, in *Chemistry of Carbon Nanotubes*, edited by V. A. Basiuk and E. Basiuk, (American Scientific Publishers, Los Angeles, CA, 2008), Vol. 2, and references cited therein.
- [11] S. P. Yadav and S. Singh, *Prog. Mater. Sci.* **80**, 38 (2016).
- [12] D. Singh, U. B. Singh, M. B. Pandey, R. Dabrowski, and R. Dhar, *Mater. Lett.* **216**, 5 (2018).
- [13] N. Dalir and S. Javadian, *J. Mol. Liq.* **287**, 110927 (2019).
- [14] S. Tomylo, O. Yaroshchuk, O. Kovalchuk, and N. Lebovka, *Phys. Chem. Chem. Phys.* **19**, 16456 (2017).
- [15] S. Schymura *et al.*, *Adv. Funct. Mater.* **20**, 3350 (2010).
- [16] D. Singh, U. B. Singh, M. B. Pandey, and R. Dhar, *Liq. Cryst.* **46**, 1389 (2019).
- [17] J. Thoen, in *Physical Properties of Liquid Crystals*, edited by D. Demus, J. Goodby, G. W. Gray, H. W. Spiess, and V. Vill (Wiley-VCH, Weinheim, 1999).
- [18] S. Singh, *Phys. Rep.* **324**, 107 (2000).
- [19] G. S. Iannacchione, *Fluid Phase Equilib.* **222-223**, 177 (2004).
- [20] E. Anesta, G. S. Iannacchione, and C. W. Garland, *Phys. Rev. E* **70**, 041703 (2004).
- [21] J. Thoen, C. Gordoyiannis, and C. Glorieux, *Liq. Cryst.* **36**, 669 (2009).
- [22] B. I. Halperin, T. C. Lubensky, and S. K. Ma, *Phys. Rev. Lett.* **32**, 292 (1974).
- [23] B. I. Halperin and T. C. Lubensky, *Solid State Commun.* **14**, 997 (1974).
- [24] G. Cordoyiannis, C. S. P. Tripathi, C. Glorieux, and J. Thoen, *Phys. Rev. E* **82**, 031707 (2010).
- [25] S. Yildiz, M. C. Cetinkaya, S. Ustunel, H. Ozbek, and J. Thoen, *Phys. Rev. E* **93**, 062706 (2016).
- [26] M. C. Cetinkaya, S. Ustunel, H. Ozbek, S. Yildiz, and J. Thoen, *Eur. Phys. J. E* **41**, 129 (2018).
- [27] K. K. Vardanyan, A. Thiel, B. Fickas, and A. Daykin, *Liq. Cryst.* **42**, 445 (2015).
- [28] J. Thoen, H. Marynissen, and W. Van Dael, *Phys. Rev. A* **26**, 2886 (1982).
- [29] M. C. Çetinkaya, S. Yildiz, H. Özbek, P. Losada-Pérez, J. Leys, and J. Thoen, *Phys. Rev. E* **88**, 042502 (2013).
- [30] K. P. Sigdel and G. S. Iannacchione, *J. Chem. Phys.* **139**, 204906 (2013).
- [31] P. Kalakonda and G. S. Iannacchione, *Phase Transit.* **88**, 547 (2015).
- [32] R. B. Rožič, E. Karatairi, G. Nounesis, V. Tzitzios, G. Cordoyiannis, S. Kralj, and Z. Kutnjak, *Mol. Cryst. Liq. Cryst.* **553**, 161 (2012).
- [33] G. Cordoyiannis, L. K. Kurihara, L. J. Martinez-Miranda, C. Glorieux, and J. Thoen, *Phys. Rev. E* **79**, 011702 (2009).
- [34] A. Mertelj, L. Cmok, M. Copic, G. Cook, and D. R. Evans, *Phys. Rev. E* **85**, 021705 (2012).
- [35] Y. Lin, A. Daoudi, F. Dubois, A. S. Mera, C. Legrand, and R. Douali, *J. Mol. Liq.* **232**, 123 (2017).
- [36] K. P. Sigdel and G. S. Iannacchione, *Eur. Phys. J. E* **34**, 34 (2011).
- [37] S. Yildiz, M. C. Cetinkaya, and H. Ozbek, *Fluid Phase Equilib.* **495**, 47 (2019).

- [38] S. Urban, in *Physical Properties of Liquid Crystals: Nematics*, edited by D. A. Dunmur, A. Fukuda, G. R. Luckhurst (Institution of Electrical Engineers, London, UK 2002).
- [39] S. Urban *et al.*, *Phys. Chem. Chem. Phys.* **5**, 924 (2003).
- [40] S. Starzonek, S. J. Rzoska, A. Drozd-Rzoska, K. Czupryński, and S. Kralj, *Phys. Rev. E* **96**, 022705 (2017).
- [41] S. J. Rzoska, S. Starzonek, A. Drozd-Rzoska, K. Czupryński, K. Chmiel, G. Gaura, A. Michulec, B. Szczypek, and W. Walas, *Phys. Rev. E* **93**, 020701(R) (2016).
- [42] S. Erkan, M. Cetinkaya, S. Yildiz, and H. Ozbek, *Phys. Rev. E* **86**, 041705 (2012).
- [43] S. Yildiz, M. C. Cetinkaya, H. Ozbek, V. Tzitzios, and G. Nounesis, *J. Mol. Liq.* **298**, 112029 (2020).
- [44] W. Maier, and G. Meier, *Z. Naturforsch. A* **16**, 262 (1961).
- [45] M. A. Anisimov, *Critical Phenomena in Liquids and Liquid Crystals* (Gordon and Breach, Philadelphia, PA, 1990).
- [46] B. Van Roie, J. Leys, K. Denolf, C. Glorieux, G. Pitsi, and J. Thoen, *Phys. Rev. E* **72**, 041702 (2005).
- [47] I. Chirtoc, M. Chirtoc, C. Glorieux, and J. Thoen, *Liq. Cryst.* **31**, 229 (2004); S. Yildiz, H. Ozbek, C. Glorieux, and J. Thoen, *ibid.* **34**, 611 (2007); M. K. Das, P. C. Barman, and S. K. Sarkar, *ibid.* **43**, 1268 (2016).
- [48] S. K. Sarkar and M. K. Das, *Phase Transit.* **89**, 910 (2016).
- [49] H. Ozbek, S. Ustunel, E. Kutlu, and M. C. Cetinkaya, *J. Mol. Liq.* **199**, 275 (2014).
- [50] A. Ranjkesh, M. Moghadam, J. C. Choi, B. Kim, J. H. Ko, M. S. Zakerhamidi, and H. R. Kim, *Phys. Chem. Chem. Phys.* **20**, 19294 (2018).
- [51] N. Sebastian *et al.*, *Phys. Chem. Chem. Phys.* **16**, 21391 (2014).
- [52] S. J. Rzoska, A. Drozd-Rzoska, P. K. Mukherjee, D. O. Lopez, and J. C. Martinez-Garcia, *J. Phys.: Condens. Matter* **25**, 245105 (2013).
- [53] S. Chakraborty, A. Chakraborty, M. K. Das, and W. Weissflog, *Phase Transit.* **92**, 806 (2019).
- [54] S. K. Sarkar and M. K. Das, *Fluid Phase Equilib.* **365**, 41 (2014).
- [55] S. K. Sarkar and M. K. Das, *Liq. Cryst.* **41**, 1410 (2014).
- [56] J. Thoen and G. Menu, *Mol. Cryst. Liq. Cryst.* **97**, 163 (1983).
- [57] P. H. Keyes, *Phys. Lett. A* **67**, 132 (1978).
- [58] J. Salud, D. O. Lopez, N. Sebastian, M. R. de la Fuente, S. D. Berart, and M. B. Ros, *Liq. Cryst.* **43**, 102 (2016).
- [59] S. Diez-Berart, D. O. Lopez, M. R. de la Fuente, J. Salud, M. A. Perez-Jubindo, and D. Finotello, *Liq. Cryst.* **37**, 893 (2010).
- [60] R. Basu and G. S. Iannacchione, *Phys. Rev. E* **81**, 051705 (2010).
- [61] L. Lisetski, S. S. Minenko, A. P. Fedoryako, and N. I. Lebovka, *Physica E* **41**, 431 (2009).
- [62] M. C. Cetinkaya, S. Yildiz, and H. Ozbek, *J. Mol. Liq.* **272**, 801 (2018).
- [63] S. Yildiz, I. Koseoglu, and M. C. Cetinkaya, *J. Mol. Liq.* **209**, 729 (2015).
- [64] A. D. Drozd-Rzoska, S. J. Rzoska, J. Ziolo, and J. Jazyn, *Phys. Rev. E* **63**, 052701 (2001).
- [65] N. Trbojevic, D. J. Read, and M. Nagaraj, *Phys. Rev. E* **96**, 052703 (2017).
- [66] H. J. Coles, in *The Optics of Thermotropic Liquid Crystals*, edited by S. Elston and R. Sambles (Taylor and Francis, London, UK, 1998), Chap. 4.
- [67] R. Basu, D. Kinnamon, and A. Garvey, *Liq. Cryst.* **43**, 2375 (2016).
- [68] Y. Lin, A. Daoudi, A. Segovia-Mera, F. Dubois, C. Legrand, and R. Douali, *Phys. Rev. E* **93**, 062702 (2016).
- [69] S. Chakraborty, A. Chakraborty, M. K. Das, and W. Weissflog, *J. Mol. Liq.* **219**, 608 (2016).
- [70] C. Grigoriadis, H. Duran, M. Steinhart, M. Kappl, H. J. Butt, and G. Floudas, *ACS Nano* **5**, 9208 (2011).
- [71] A. Selevou, G. Papamokos, M. Steinhart, and G. Floudas, *J. Phys. Chem. B* **121**, 7382 (2017).
- [72] M. Mishra, R. S. Dabrowski, J. K. Vij, A. Mishra, and R. Dhar, *Liq. Cryst.* **42**, 1580 (2015).
- [73] Z. Kutnjak, S. Kralj, G. Lahajnar, and S. Zumer, *Phys. Rev. E* **68**, 021705 (2003).
- [74] P. van der Schoot, V. Popa-Nita, and S. Kralj, *J. Phys. Chem. B* **112**, 4512 (2008).
- [75] V. Popa-Nita and S. Kralj, *J. Chem. Phys.* **132**, 024902 (2010).
- [76] S. V. Burylov and Y. L. Raikher, *Phys. Rev. E* **50**, 358 (1994).
- [77] D. Črešnar, C. Kyrou, I. Lelidis, A. D. Rzoska, S. Starzonek, S. J. Rzoska, Z. Kutnjak, and S. Kralj, *Crystals* **9**, 171 (2019).
- [78] R. Verma, M. Mishra, R. Dhar, and R. Dabrowski, *Liq. Cryst.* **44**, 544 (2017).
- [79] R. Verma, M. Mishra, R. Dhar, and R. Dabrowski, *J. Mol. Liq.* **221**, 190 (2016).
- [80] A. Shah, M. S. Sannaikar, S. R. Inamdar, B. Duponchel, R. Douali, and D. P. Singh, *J. Lumin.* **226**, 117509 (2020).
- [81] N. Dalir and S. Javadian, *J. Mol. Liq.* **341**, 117287 (2021).
- [82] Ch. Kartikeswar Patro, R. Verma, A. Garg, R. Dhar, and R. Dabrowski, *Liq. Cryst.* **48**, 345 (2021).
- [83] D. P. Singh *et al.*, *J. Mol. Liq.* **302**, 112537 (2020).
- [84] Y. Lin *et al.*, *RSC Adv.* **7**, 35438 (2017).
- [85] S. Orlandi *et al.*, *Phys. Chem. Chem. Phys.* **18**, 2428 (2016).
- [86] A. Ranjkesh, M. Cvetko, J. C. Choi, and H. R. Kim, *Phase Transit.* **90**, 423 (2017).
- [87] N. Dalir and S. Javadian, *J. Appl. Phys.* **123**, 115103 (2018).
- [88] G. V. Varshini, D. S. Shankar Rao, P. K. Mukherjee, and S. K. Prasad, *J. Phys. Chem. B* **122**, 10774 (2018).
- [89] J. Kumar, V. Manjuladevi, R. Kumar Gupta, S. Kumar, *Liq. Cryst.* **42**, 361 (2015).
- [90] N. Yadav, R. Dabrowski, and R. Dhar, *Liq. Cryst.* **41**, 1803 (2014).
- [91] A. S. Pandey, R. Dhar, S. Kumar, and R. Dabrowski, *Liq. Cryst.* **38**, 115 (2011).
- [92] S. K. Prasad, M. V. Kumar, T. Shilpa, and C. V. Yelamaggad, *RSC Adv.* **4**, 4453 (2014).
- [93] P. C. Menon, R. N. Rajesh, and C. Glorieux, *Rev. Sci. Instrum.* **80**, 054904 (2009).
- [94] P. R. Bevington and D. K. Robinson, *Data Reduction and Error Analysis for the Physical Sciences*, 3rd ed. (McGraw Hill, New York, NY, 2003).
- [95] A. Żywociński, *J. Phys. Chem. B* **107**, 9491 (2003).
- [96] A. Chakraborty, S. Chakraborty, and M. K. Das, *Phys. B: Condens. Matter* **479**, 90 (2015).
- [97] S. K. Sarkar, A. Chakraborty, and M. K. Das, *Liq. Cryst.* **43**, 22 (2016).
- [98] N. Sebastian *et al.*, *J. Phys. Chem. B* **115**, 9766 (2011).
- [99] D. S. Simeão and M. Simoes, *Phys. Rev. E* **86**, 042701 (2012); M. Simões and D. S. Simeão, **74**, 051701 (2006).

- [100] M. Simões, D. S. Simeao, and S. M. Domiciano, *Mol. Cryst. Liq. Cryst.* **576**, 76 (2013); D. S. Simeão and M. Simoes, **576**, 88 (2013).
- [101] M. Simões, D. S. Simeao, and K. E. Yamaguti, *Liq. Cryst.* **38**, 935 (2011).
- [102] J. Thoen, G. Cordoyiannis, P. Losada-Perez, C. Glorieux, *J. Mol. Liq.* **340**, 117204 (2021).
- [103] K. K. Chan, M. Deutsch, B. M. Ocko, P. S. Pershan, and L. B. Sorensen, *Phys. Rev. Lett.* **54**, 920 (1985).
- [104] A. Chakraborty, S. Chakraborty, and M. K. Das, *Phys. Rev. E* **91**, 032503 (2015).
- [105] J. J. Binney, N. J. Dowrick, A. J. Fisher, and M. E. J. Newman, *The Theory of Critical Phenomena* (Clarendon Press, Oxford, UK, 1992).
- [106] A. Żywociński and S. A. Wiczorek, *J. Phys. Chem. B* **101**, 6970 (1997).
- [107] A. Zywockinski, S. A. Wiczorek, and J. Stecki, *Phys. Rev. A* **36**, 1901 (1987).
- [108] C. W. Garland and G. S. Iannacchione, *J. Phys. Chem. B* **113**, 3901 (2009).
- [109] G. S. Iannacchione, S. Park, C. W. Garland, R. J. Birgeneau, and R. L. Leheny, *Phys. Rev. E* **67**, 011709 (2003).
- [110] K. Denolf, B. Van Roie, C. Glorieux, S. Yildiz, H. Ozbek, and J. Thoen, *Mol. Cryst. Liq. Cryst.* **477**, 3 (2007).
- [111] K. P. Sigdel and G. S. Iannacchione, *Phys. Rev. E* **82**, 051702 (2010).
- [112] D. W. Berreman and S. Meiboom, *Phys. Rev. A* **30**, 1955 (1984).
- [113] P. Kalakonda, R. Basu, I. R. Nemitz, C. Rosenblatt, and G. S. Iannacchione, *J. Chem. Phys.* **140**, 104908 (2014).
- [114] G. S. Iannacchione, C. W. Garland, J. T. Mang, and T. P. Rieker, *Phys. Rev. E* **58**, 5966 (1998).
- [115] S. Pawlus, J. Osinska, S. J. Rzoska, S. Kralj, and G. Cordoyiannis, in *Soft Matter Under Exogenic Impacts*, edited by S. J. Rzoska and V. A. Mazur (Springer, Netherlands, 2007).
- [116] G. V. Varshini, D. S. Shankar Rao, P. K. Mukherjee, and S. K. Prasad, *J. Mol. Liq.* **286**, 110858 (2019).
- [117] R. J. Mandle and J. W. Goodby, *Liq. Cryst.* **44**, 656 (2017).
- [118] U. Zammit, M. Marinelli, F. Mercuri, S. Paoloni, and F. Scudieri, *Rev. Sci. Instrum.* **82**, 121101 (2011).